Synthesis and testing of porous carbon composites supported catalysts for environmental and refining applications

A thesis submitted to

Indian Institute of Science Education and Research (IISER), Pune;

in partial fulfilment of the requirements for the

BS-MS Dual Degree Programme

Madhusudhan Naik. J

(Reg. No: 20101050, 5th year BS-MS)

Thesis Supervisor

Dr Madhusudhan Rao

Centre for Novel & Catalytic materials (CNCM),

Shell Technology Centre Bangalore

March 2016

Certificate

This is to certify that this dissertation entitled "**Synthesis and testing of carbon composites supported catalysts for environmental and refining applications**" towards the partial fulfilment of the **BS-MS dual degree** programme at the Indian Institute of Science Education and Research, Pune represents original research carried out by **Madhusudhan Naik Jarpla** at Shell Technology Centre Bangalore, India under the supervision of "Dr. Madhusudhan Rao, Senior Process Researcher, Centre for Novel & Catalytic materials (CNCM)"during the academic year **2015-2016**.

Signature of the Supervisor
(Dr Madhusudhan Rao)

Date: 24/03/2016
Place: Bangalore

Declaration

I hereby declare that the matter embodied in the report entitled "**Synthesis and testing of carbon composites supported catalysts for environmental and refining applications**" are the results of the investigations carried out by me at the Centre for Novel & Catalytic materials (CNCM) department, **Shell Technology Centre Bangalore, India**, under the supervision of Dr Madhusudhan Rao and the same has not been submitted elsewhere for any other degree.

Madhusudhan Naik
Signature of the Student

(Madhusudhan Naik. J)

Date: 24/03/2016

Place: Bangalore

Acknowledgements

I would like to thank Dr. Laxmi Narasimhan, General Manager, Centre for Novel &Catalytic Materials (CNCM), Shell Technology Centre Bangalore for giving me this internship opportunity which introduced me to different areas of Industrial catalytic research. I would like to express my sincere gratitude to my advisor Dr. Madhusudhan Rao for his guidance and continuous support throughout my project. I thank him for his concern and interest in helping me complete this thesis. I would be grateful to Veena for her support and help till the end of my project. I take this opportunity to thank my labmates Ashutosh, Sireesha, Vedant, Dr. Rikesh, Amita and Dr. Dhairya for their valuable insights and discussions. I am thankful to everyone in the CNCM group for being friendly and helpful. I thank Gaurav rayal for helping me with the SEM images. I would like to thank my TAC member Dr. Vaidhyanathan, IISER Pune for his valuable comments and suggestions. Finally I would like to thank my parents for encouraging me throughout my studies.

Contents

List of figures

List of tables

Abstract

Porous carbon-TiO_2 & carbon-Al_2O_3 composite supports were prepared and tested for NO reduction via NH_3-SCR and hydrotreating of vacuum gas oil (VGO) respectively. The effects of type of porous carbon (activated carbon, graphite, and carbon black), amount of carbon loading and calcination temperatures on the textural properties of carbon-TiO_2 & Al_2O_3 composite supports prepared by mulling and extrusion were studied. Using high surface area porous carbons with TiO_2 precursors significantly increased the surface area and pore volume of supports calcined at 300^{o}C. The % NO reduction of x wt% V_2O_5/ (10 & 30 wt%) Carbon-TiO_2 catalysts calcined at 300^o C shows significant higher (> 50 %) activity than the reference catalyst in absence of H_2O. This increase in catalytic activity can be attributed to combined contribution from increased dispersion of V_2O_5 on the supports, reduced diffusion limitations of NH_3-SCR reaction and surface functional groups on porous carbons acting as catalyst. In case of Carbon-alumina composites textural properties were minimally affected at low carbon loadings (≤30wt%) at different calcination temperatures. Carbon black-alumina composites supported NiMo catalysts tested for hydrotreating of vacuum gas oil (VGO) shows activity comparable to reference catalysts. Activated carbon-alumina composites show decrease in catalytic activity which could be due to sintering of NiMoS phase into large crystals thus reducing the number of active sites.

1.0. Introduction

Rising concerns on the effects of air pollution on environment and health resulted in increasing interest in developing new technologies to either regulate the emissions or to produce low sulfur and nitrogen containing fuels. Major constituents of air pollution are Nitrogen oxides (NO_x), CO, SO_2 and volatile organic compounds (VOC). NO_x is a generic term for NO, NO_2 and N_2O. Nitric oxide (NO), nitrogen dioxide (NO_2) are toxic and also contribute to formation of acid rains and smog, while nitrous oxide (N_2O) contributes to global warming and depletion of ozone layer[1]. Major sources of NO_x and SO_2 emission are from fuel combustion (oxidation of organic nitrogen, sulfur contaminants in fuel) in automobiles and industrial flue gases[2].

Catalytic technologies are the most attractive solutions to reduce the environmental emissions because of its high efficiency and low-cost[3]. A catalyst is a substance that increases the rate of chemical reaction without getting appreciably consumed in the process. In general a site on the catalyst forms complex with the reactants and products are formed. Heterogeneous catalysis involves the catalysts and reactants/products present in different phases, typically reactants in gas phase are contacted with solid catalyst material at elevated temperature and sometimes at high pressures. Catalysts are present in all key industrial sectors such as production of chemicals, in emission abatement, energy transformation[4].

Industrial catalysts comes in several shapes and forms (extrudates, pellets, monoliths etc.) and consisting of different components. Fig 1 shows different components of a heterogeneous catalyst[5]. First there is **porous support** material to ensure the structural integrity of the catalyst and to increase the surface area available for the reaction. **Active phase** (metals or metal oxides) is deposited on the support material which provides sites for the reaction to occur. **Promoters** can be used to enhance the catalytic performance and stability[6].

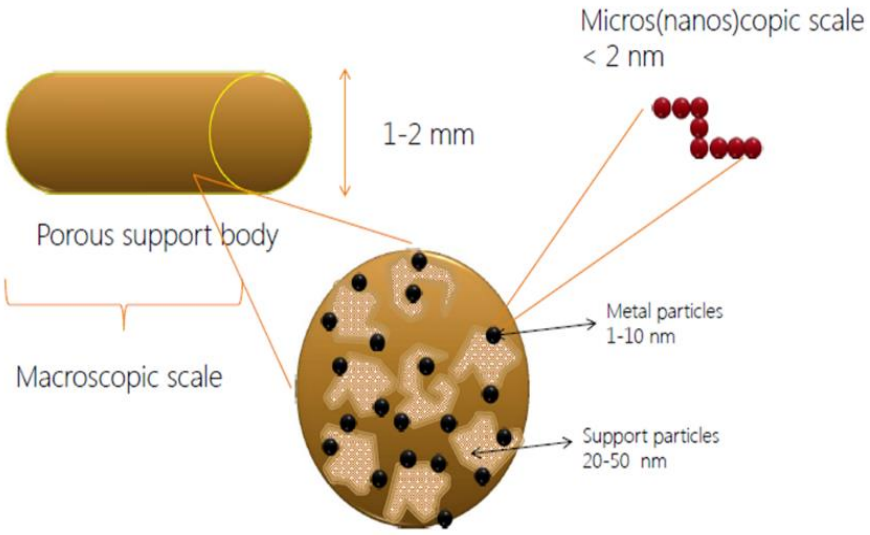

Fig.1. Basic components of a heterogeneous catalyst (Ref.5)

1.1 NOx reduction by NH3-SCR:

Our focus has been on NO removal from industrial effluent streams. In order to meet the strict environmental legislations, great efforts have been taken to either limit NO formation or to convert them into Nitrogen (N_2).

Selective catalytic reduction (SCR):

The SCR process was first developed in Japan in 1970s and is most successfully developed technology to reduce NO_x emissions. It involves selective reduction of NO_x to N_2 in presence of oxygen and a reducing agent (NH_3) using TiO_2 supported V_2O_5 catalyst monolith. Other reducing agents like methane, propane and urea have also been used[7]. NH_3 is considered as preferable reducing agent because of its relatively high N_2 selectivity (One atoms of N_2 molecule come from NO and one from NH_3) and high activity[8]. Major reactions occurring on the surface of the catalysts during the NH_3-SCR process are as follows:

$$4NH_3 + 4NO + O_2 \longrightarrow 4N_2 + 6\,H_2O \text{ (standard SCR reaction)}$$

$$4NH_3 + 2NO + 2NO_2 \longrightarrow 4N_2 + 6\,H_2O \text{ (fast SCR)}$$

$$4NH_3 + 2\,NO_2 + O_2 \longrightarrow 3N_2 + 6\,H_2O$$

The fast SCR reaction involves both NO and NO_2 (1:1 ratio), exhibit a reaction rate at least ten times faster than a standard SCR reaction. Many undesirable side reactions with different stoichiometries result in formation of N_2O, NO and NO_2 decreasing the

selectivity of N_2 formation. While treating emissions from sulfur containing fuels or industrial flue gases with SO_2 content, fouling of the active sites takes place due to SO_2 oxidation. If the operating temperature is below the dew point (250°C) of ammonium sulfates, ammonium bisulfate condenses in the pores of the catalyst, resulting in severe loss of deNOx activity.

$$2SO_2 + O_2 \longrightarrow 2SO_3$$

$$2NH_3 + SO_3 + H_2O \longrightarrow (NH_4)_2SO_4$$

$$NH_3 + SO_3 + H_2O \longrightarrow NH_4HSO_4$$

Conventional honeycomb SCR systems are based on TiO_2 supported V_2O_5-WO_3 catalysts. TiO_2-anatase is considered as best support than any other metal oxides due to its high activity and low sensitivity towards SO_2 poisoning. TiO_2 supports are weakly and reversibly sulfated under SCR conditions. Vanadium oxides (V_2O_5) disperses well on TiO_2 support and offers high activity and excellent N_2 selectivity[9]. However these catalysts require high operating temperatures (300 – 400^{o}C) which restricts the retrofit of SCR systems to upstream of sulfur and particulate removal device[10]. As it is not economical to install the SCR systems upstream due to limited space and access. Therefore **low temperature NO_x reduction** is of particular interest, due to its convenience of retrofitting at the tail end of the systems and low energy consumption avoiding the need for further heating of flue gas emissions before entering the SCR catalyst. The typical constituents of flue gases at the tail end of waste incineration plants are NO_x, SO_2, H_2O, O_2 [13].

Increasing SCR activity for low temperature (≤ 250^{o}C) NO removal along with high N_2 selectivity (eliminating the formation of N_2O, NO, NO_2) and low deactivation rate is still a challenge for catalyst technologies. Our focus has been to increase the catalytic activity of a NH_3- SCR catalyst for low temperature NO reduction applications.

Catalytic activity mainly depends on surface properties of the supports (TiO_2), composition and dispersion of catalytic phases (V_2O_5) loaded and diffusion of reactants and products (in case of diffusion limited reactions) through the porous support[14-15]. In this project focus has been on increasing the catalytic activity of NO reduction catalyst by increasing the surface area & tuning pore structure of the supports. An increase in surface area helps in better dispersion and stabilization of

catalyst on support surface, resulting in more active sites available for the reaction. Pore structure can be modified by various methods such as doping with different metal-oxides, use of inorganic (porous carbons) or water-soluble organic polymers (cellulose) as combustible additives and varying calcination temperatures[16-18]. Different porous carbons have been used as additives to modify pore structure of supports and improving textural properties of supports by varying carbon content and calcination temperatures. Since the NO reaction reaction is diffusion limited reaction[19], catalytic activity also depends on rate of diffusion of reactants (NH_3, NO_x) through the pore structure of supports, rate of reaction at the active sites, and rate of diffusion of products (N_2, H_2O). The use of porous carbons can reduce the diffusion limitations for the NO reduction reaction.

1.2. Hydroprocessing of Vacuum gas oil (VGO):

In recent years there has been great interest in producing low sulfur and nitrogen containing fuels. Fig.2 shows various stages in crude oil refining. Hydroprocessing includes hydrotreating and hydrocracking. Hydrotreating involves removal of impurities such as hetero atoms and metal containing compounds from feed during various stages of oil refining. Hydrocracking involves breaking of long C-C chains into smaller fragments. The various nitrogen and sulfur containing compounds present in the vacuum gas oil are shown in fig 3a& 3b. The combustion of these sulfur and nitrogen containing compounds produces NO_x and SO_2 which are dangerous for environment. Therefore N- containing and S-containing groups are removed by hydrogenation reactions using specific processes known as Hydrodesulfurization (HDS), Hydrodenitrogenation (HDN)[20].

Hydrotreating catalysts consists of alumina supported Mo-based sulfide catalysts with Ni or Co sulfides used as promoters. The active phase of catalysts consists of MoS_2 slabs (or (Ni)MoS_2 phase) in the form of stacked layers. The (Ni)MoS_2 slabs distribution on the support depends on impregnation conditions, acidity of the supports, sulfiding and operating conditions. Under reaction conditions the corner and edge sites of $NiMoS_2$ are unstable and can be removed. Thus resulting in the formation of sulfur vacancies (or coordinatively unsaturated sites) at corner and edge sites of (Ni)MoS_2. These sites are Lewis acidic and can adsorb molecules with unpaired

electrons (from N- and S- containing compounds in feed). They can also activate hydrogen forming Mo-H and S-H species which subsequently gets transferred to reacting molecules releasing H_2S and NH_3.

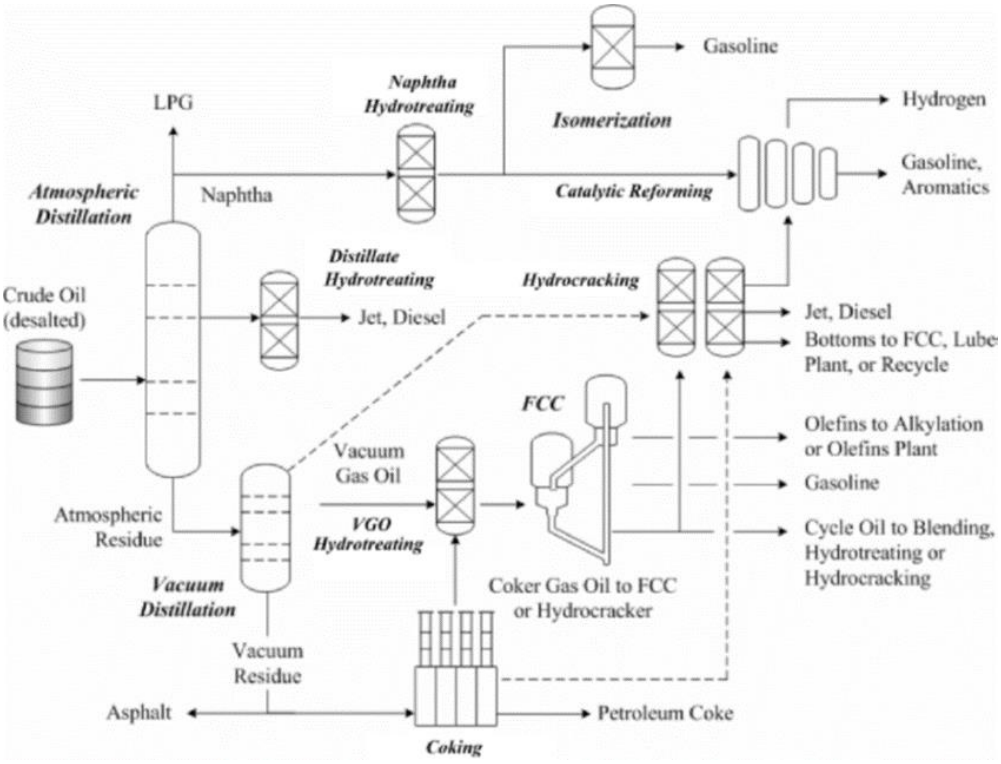

Fig 2: Schematic of various stages of crude oil refining (Ref. 19)

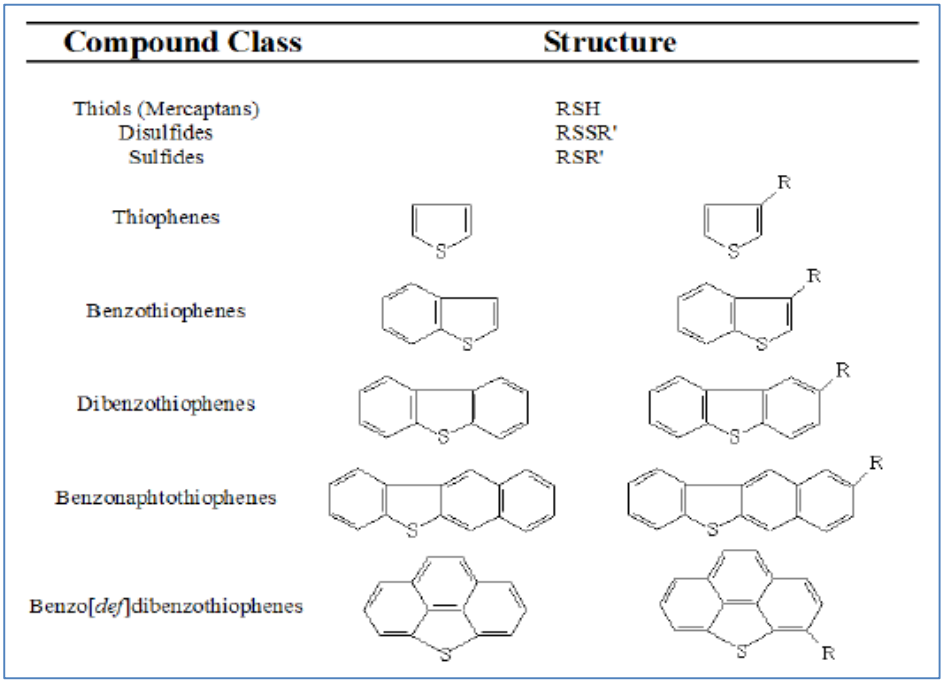

Fig 3a. Sulfur containing compounds in crude oil (Ref.20)

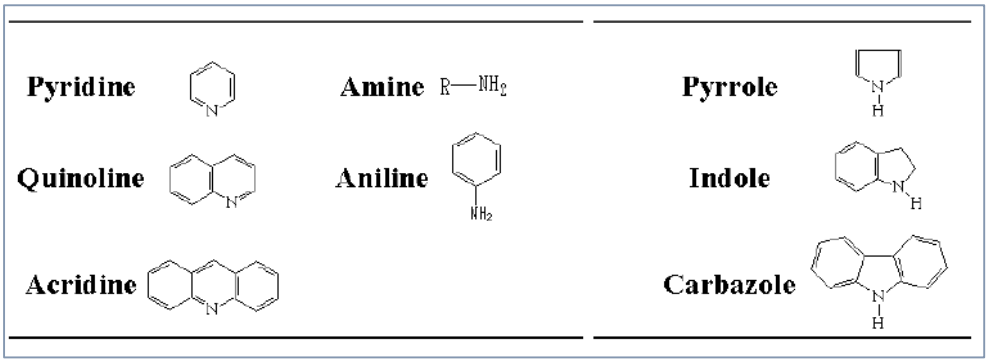

Fig 3b. Nitrogen containing compounds in crude oil (Ref. 20)

Alumina is considered as best support because of its high surface area (200-300 m^2/g), affinity to sulfides and mechanical strength. Catalytic activity of hydroprocessing depends on pore size, metal-support interaction, acidity of the support, dispersion of active phase on support. The N-containing compounds adsorb strongly on active sites thereby blocking other compounds (S-containing) to adsorb and restrict hydrogen activation. The catalytic activity is also lost due to coking and deposition of metals (V and Ni compounds)[20].

Our focus has been on modifying pore structure using different porous carbon-alumina composites as supports. High surface area and hierarchical pore structures in (100-250 Å) range are known to increase the catalytic activity by providing more sites for active phase deposition as well as allowing larger S- and N- containing molecules to diffuse inside the pore structure and react faster[22-23]. Activated carbon-alumina composites have been reported to increase the surface properties and catalytic activity for HDS of dibenzothiophene[24]. Since carbon is neutral (at pH = PZC) it would have weak metal-support interaction thereby forming taller stacking layers of MoS_2 slabs. The taller stacking can result in more active Mo-S bonds thereby forming more number of active sites for reaction. The effect of carbon-alumina composite supports on HDN and HDS activity of vacuum gas oil (VGO) were studied.

1.3 Porous carbons as composite supports:

Porous carbons (Activated carbon & Graphite) can be used as support materials in catalysis since they have high surface areas. Activated carbons process large number of micropores and high surface area. As they are prepared from feedstock (coconut-shell and wood based) by pyrolysis to drive off all volatiles producing char with high carbon content, subsequent activation in oxidizing medium at high temperatures (800 K-1400 K) results in high surface area carbons. During activation CO, CO_2, H_2 are released resulting in the formation of pores[25].

Structure and surface chemical properties of supports are considered as important parameters in governing the rate of catalytic activity. The porous carbons (Activated carbon and Graphite) have graphitic structure. There exists unsaturated carbon atoms at the edges of graphene layers and defects in basal plane, which make these sites susceptible to react with oxygen, hydrogen and nitrogen in various proportions. Thus resulting in formation of variety of surface functional groups (acidic and basic) at the edges of graphene sheets and at the defect centers[26] as shown in fig 4. Carbon materials in aqueous solutions are neutral, as they have both acidic and basic surface groups. The acidic surface groups donate protons into the solution (surface becomes negatively charged) and basic groups accept protons from the solution (surface becomes positively charged). At certain pH the net surface charge is zero, which is called pH at point of zero charge (PZC). The surface functional groups are typically characterized by point of zero charge (PZC) measurements. If the solution pH > PZC the surface becomes negatively charged (due to deprotonation of acidic groups). Whereas if pH < PZC the surface becomes positively charged (due to protonation of basic groups). Based on PZC of porous carbons, they can be also act as sites for anchoring active metal complexes (on choosing oppositely charged metal precursor solution) or can itself act as catalysts[27].

Carbon black can also be used as additive to the precursors during support preparation. The pore size distribution and pore volume of the supports can be tuned by selection of type carbon black and controlling the quantity of addition. Carbon black has a tendency to form chained structures with particles linking together. The chain length of different carbon blacks can be estimated from dibutyl phthalate (DBP)

adsorption[28]. Upon burning carbon black content completely results in pore networks formation with voids left by chained carbon black particles.

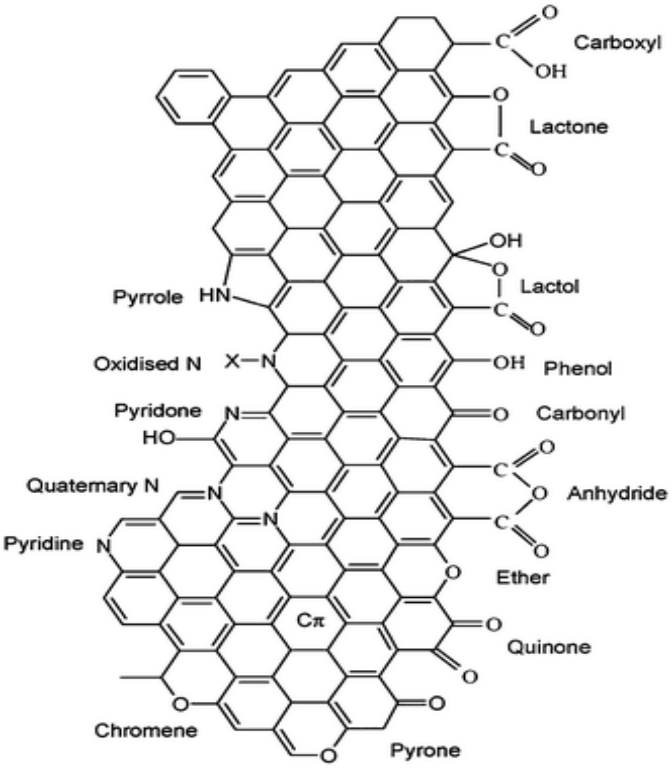

Fig 4. Nitrogen and oxygen containing surface functional groups on porous carbons.

Acidic functional groups: carboxylic acid, lactones, Phenol, anhydride

Basic functional groups: Nitrogen containing groups, π electrons in the basal plane

Ref: 26

Therefore the use of porous carbons during support preparation could be advantageous as-

- They can produce highly dispersed and stabilized active phases on supports thereby increasing the catalytic activity
- High surface area porous carbons can reduce diffusion limitations of reaction by providing easy access of reactants to the active sites of catalyst.
- The surface functional groups (if present) on porous carbons can also provide sites for anchoring of active metal complexes or the porous carbon can itself act as catalyst.

Considering all these aspects, we used different porous carbon sources (Activated carbon, Graphite, Carbon black) to prepare C-TiO_2 & C-Al_2O_3 composite supports by process called mulling and extrusion. All the prepared C-TiO_2 composite supports were impregnated with active metals V_2O_5 & C-Al_2O_3 composite supports were impregnated with MoO_3 and tested for their catalytic activity.

The scope of our work is –

- Synthesize a suite of C-TiO_2 and C-Al_2O_3 composite supports processing a range of surface areas, pore diameters and pore volumes.
- To study the effect of different porous carbons loadings and calcination temperatures in tuning the pore structure of TiO_2 & Al_2O_3 supports by either retaining or completely burning out the carbon content.
- To study the effect of these C-TiO_2 and C-Al_2O_3 composite supports on the catalytic activity of low temperature SCR of NO and hydrotreating of vacuum gas oil (VGO) respectively.

2.0. Methods and Materials:

2.1. Mulling and extrusion:

Carbon-TiO_2 and carbon-Al_2O_3 composite supports were prepared by 'mulling and extrusion'. Mulling is a process of preparation of porous materials by peptization, which involves kneading of powder precursors into a smooth paste and then extrusion through a pierced die. The base components are metal oxide/hydroxide powder precursors, water, an acid (peptizing agent) and rheological additives. First calculated amounts of base components are added to the kneading machine (muller) and mix-mulled. During the process, powder precursors gets peptized and evolve into a smooth paste. Preparation of extrudable smooth paste involves adjusting right amount of water and acid[29].

Various parameters needs to be considered during mulling process which ultimately affect the surface properties of the support materials, like amount of water, type of acid and quantity of acid etc. If quantity of water added exceeds a certain limit, mulled paste exudes water making it difficult to extrude.

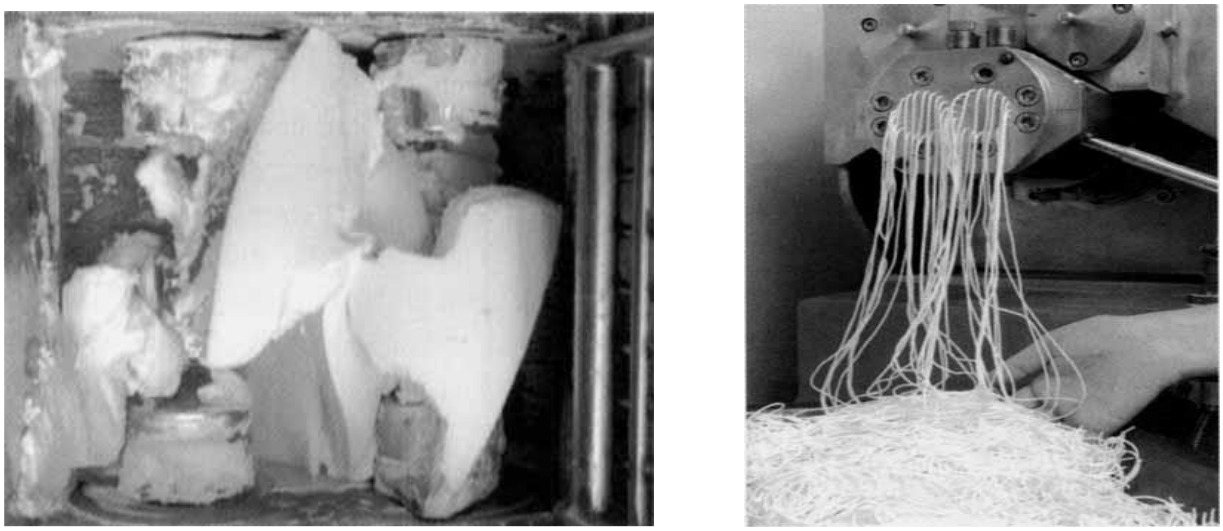

Fig.5: a) Wet acidified paste formed during mix-mulling and b) Extrusion process (Ref. 28)

Also, if amount of acid added above critical value dough tends to dissolve leading to a sticky paste making it difficult to move along the extruder barrel.

Basic theory behind the physical and chemical process governing mulling and extrusion is as follows: Powder precursors (metal oxides/hydroxides) taken for mix-mulling consists of agglomerates which are made up of aggregates held together by

weak interactions (vanderwaals forces, hydrogen bonding). These aggregates are bound by chemical bonds (i.e,oxo-bridges), which in turn are made of primary particles linked together in clusters. The primary particle clusters correspond to ultimate level of dispersion. Fig.6 & 7 shows the schematic of powder precursor constituents (agglomerates and aggregates) along with corresponding pore volumes. During mulling, agglomerates break down into separate aggregates due to the shear stress of rotating blades (i.e. hydrogen bonds are broken) of muller. But inorder to bring deaggregation physical action is not enough, since it involves breaking of chemical bonds (oxobridges). Therefore acids are used to break aggregates into particle clusters. Because acid addition protonates the surface hydroxyl groups resulting in the stable dispersion of particles due to repulsion. This method of producing a stable dispersion of particles is called **peptization.** During the process, powder agglomerates (macropores >50 nm) break down into primary particles (mesoporous < 50 nm) by shear stress and acid attack[29].

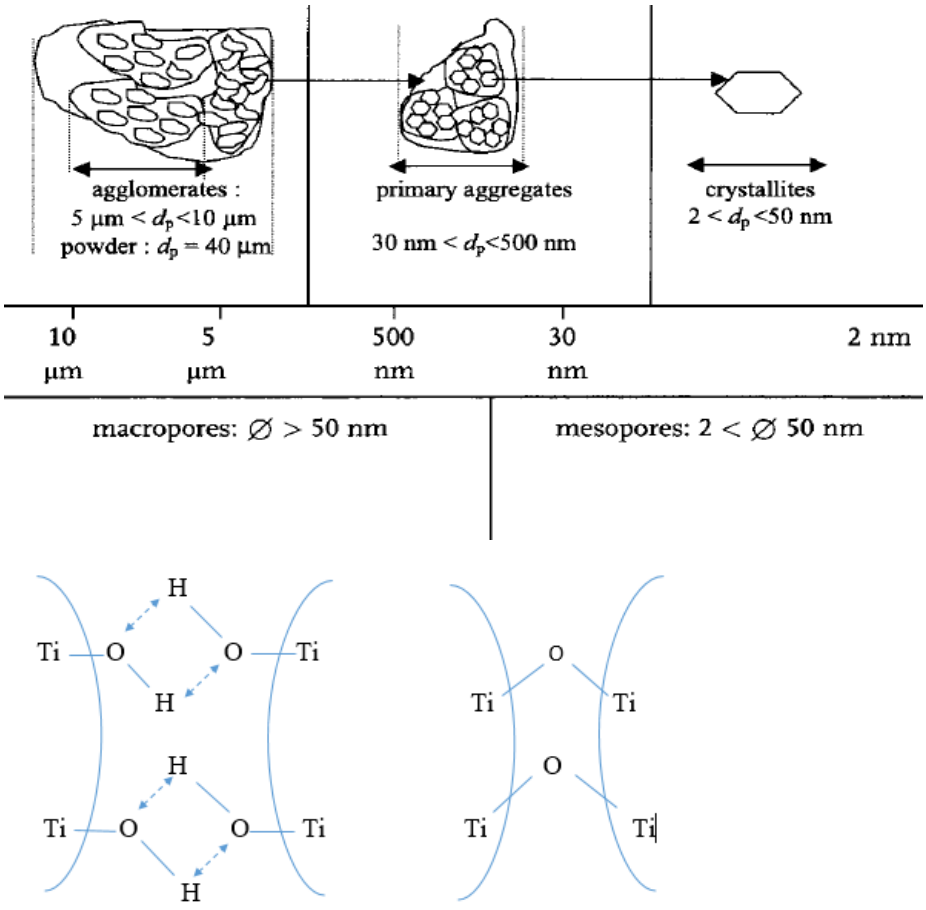

Fig.6: Schematic of powder precursor constituents along with corresponding pore volumes (Ref.28)

Fig.7: Titania precursor powder agglomerates (bound by hydrogen bonds) and aggregates bound by chemical bonds (oxobridges)

2.1. Preparation of C-TiO_2 and C-Al_2O_3 composite supports by Mulling and Extrusion.

Different C-TiO_2 and C-Al_2O_3 supports with varying carbon content were prepared. The required amount of carbon and metal oxide/hydroxides precursors for producing desired composites were calculated. After addition of powder precursors in the mulling chamber calculated amounts of acid and combustible organic polymers were added and dry mixed for certain duration. This was followed by addition of required quantity of water. The mixture was then mulled for to obtain a smooth paste.

The mix-mulled paste was then extruded to produce shaped extrudates. The obtained C-TiO_2 extrudates were then dried and calcined at 300^o C and 500^o C/1 hr and C-Al_2O_3 extrudates were dried and calcined at 500 ^{o} C and 600 ^{o} C/2hr. During drying process free water is removed and during calcination dehydroxylation and combustion of carbon as CO_2 take place resulting in formation of porous C-TiO_2 and Al_2O_3 supports.

Porous carbons precursors

Three different carbons (Activated carbon, Graphitic carbon and carbon black) have been used to prepare 10 wt% and 30 wt % Carbon- TiO_2 extrudes for deNOx application and 10-40 wt% Carbon- Al_2O_3 were prepared for hydroprocessing applications. All the carbon sources were procured from a third party vendor. These carbons differ greatly in their surface area and pore volumes as shown in Table.1. Carbon black (CB) has DBP adsorption strength of 114 (cc/100g) value as provided by vendor.

Carbon Source (Grade)	BET surface area (m2/g)	t-plot Micropore Area (m2/g)	Pore Volume (cm3/g)
Activated Carbon (AC)	1200	360	0.82
Graphitic carbon (GC)	408	122	0.47
Carbon black (CB)	110	10	0.88

Table 1: Three different Porous carbon sources used for preparing Carbon-TiO_2 supports

2.2. Impregnation of active metals on porous C-TiO_2 and C-Al_2O_3 supports:

After calcination, C-TiO_2 & C-Al_2O_3 supports were impregnated using acidified aqueous active metal precursor solution by conventional pore volume impregnation method[30]. The supports gets impregnated with active metals by capillary action and electrostatic interaction. After impregnation, catalysts were dried and calcined.

2.3. Catalyst testing:

a) For low temperature deNOx activity:

Prepared V_2O_5/Carbon-TiO_2 composite catalysts were crushed and sieved before testing. Carbon-TiO_2 supports with only two different grades (AC, GC) have been tested for their low temperature NOx reduction (in the absence of H_2O & presence of H_2O) ability using NH_3 as reducing agent. Flue gas used for testing comprises of NO, NH_3, SO_2, H_2O, O_2 and balance-Ar. Temp: 120-180^{0}C. The concentrations of NO, NO_2 and O_2 at the inlet and outlets were measured simultaneously using online flue-gas analyzer.

b) For hydroprocessing of vacuum gas oil (VGO) :

Prepared Mo-Ni-oxide catalysts supported on different carbon-alumina composites are tested for Hydrodesulfurization (HDS), Hydrodenitrogenation (HDN) activity of VGO in trickle bed flow reactor. Catalysts were sulfided using straight run gas oils

spiked with sulfur compound to convert metal oxides to metal sulfides. The collected samples were analyzed for sulfur and nitrogen content (ppm) by elemental analyzer.

2.4. Measurement of surface properties:

The textural properties of the samples were analyzed by N_2 adsorption at 77K using Micromeritics Tristar II instrument. All the samples were preheated at 150^o C for 3hrs under N_2 flow before analysis. The principle of analysis is based on physisorption of adsorptive (N_2) at 77K on to the surface of materials by which surface area, pore volume, pore size distribution can be measured based on different theories and their relevant equations.

Surface area of the supports are calculated using Brunauer–Emmett–Teller (BET) equation[32]-

$$1/ [v (P_0/P)-1)] = (1/v_m C) + [(C-1)/v_m C] (P/P_0)$$

Where v is adsorbed gas quantity, v_m is monolayer adsorbed gas quantity, P/P_0 is relative pressure (P and P_0 are equilibrium and saturation vapor pressure of adsorptive at given temperature), C is BET constant which is related exponentially to the enthalpy of adsorption of first and subsequent layers. From the linear plot between $1/ [v (P_0/P)-1)]$ and (P/P_0), monolayer adsorbed gas quantity (v_m) can be calculated. The total BET surface area can be determined from the values of v_m and molecular cross-sectional area of adsorptive a_m (a_m for N_2 at 77K is 0.162 nm^2) by using the equation-

$\mathbf{S_{Total} = (v_m * L * a_m)/V}$ (where L = Avogadro number and V= molar volume of adsorbed gas)

Using Barett-Joyner-Halenda method (BJH) method pore size distribution has been measured which is based on modified Kelvin equation[33]. N_2 desorption branch of isotherm has been used to estimate the pore size using amount of adsorbate evaporated from the pores of the material as the relative pressure (P/P_0) is decreased from high to low value. t-plot method has been used to determine the micropore volume & thickness of adsorbate, in which plot between volume of gas adsorbed and thickness of multilayer adsorbate formed (V vs t) is compared with a standard non-porous solid reference plot[34,35].

Using N_2 at 77K as an adsorptive for analysis of surface area and pore sizes has a limitation. In that it cannot be used for quantitative estimation of micropores (pore size < 2 nm) and ultra-micropores (<0.7 nm). N_2 is dimeric and exhibit certain specific interactions with the narrow pore walls of micropores due to its quadrapole moment. Therefore using N_2 as adsorptive does not give correct estimate of micropore surface analysis. Alternatively Argon (Ar) at 87K can be used as adsorptive for micropore analysis because of its weaker condensate-pore wall attractions in micropores[36]. Thus pore filling and analysis of ultra-micropores (<0.7nm) can also be possible using Argon.

2.5. TGA analysis:

Thermo gravimetric analysis (TGA) measures amount of weight loss as a function of increasing temperatures has been carried out on pure carbon sources to determine the calcination temperatures needed for completely burning the carbon content. TGA analysis of Carbon- TiO_2 extrudates calcined at 300^o C and 500^o C for 1 hr were carried out to determine the percentage of carbon remaining in the samples after the calcination. All the samples were heated till 700 ^{o} C at ramp rate of 10 ^{o} C/min in air to determine the percentage weight loss of carbon due to combustion releasing CO_2. (TGA results are not included due to space constraint)

2.6. SEM analysis

Scanning electron microscope (SEM) images of catalyst extrudates were taken in FEI Nova-NanoSEM 430 FEG-SEM instrument under high vacuum conditions and using 10 KeV electron beam voltage. Extrudates were fractured with knife before placing on the sample holder.

3. Results and discussion;

3.1.1 Textural characterization of Carbon-TiO_2 supports

a) *Activated Carbon (AC) -TiO_2 extrudates:*

Fig. 9 shows the N_2 physisorption isotherm plots of all Carbon (AC) -TiO_2 extrudates calcined at different temperatures. Relative pressure (P/P_o) has been plotted against quantity of gas adsorbed (mmol/g). The first step in analyzing of physisorption isotherm is to identify the isotherm type and hence the nature of the adsorption process: monolayer-multilayer adsorption, capillary condensation or micropore filling. Adsorption and desorption curves of all the samples show a characteristic hysteresis which is typical of type IV isotherm. In which capillary condensation of mesopores (pore size 2-50 nm) takes place over a range of high relative pressure (P/P_o). The initial part of the isotherm can be attributed to monolayer-multilayer adsorption and follows the same path during adsorption and desorption of the adsorptive (N_2). Hysteresis loop has been identified as H2 type based on the IUPAC classification hysteresis loops & depending upon shape of hysteresis branches[37]. The reason for hysteresis behavior is because capillary condensation during adsorption depends on the thickness of multilayer adsorbate, while capillary desorption depends on vapor-liquid equilibrium transitions. H2 type of hysteresis have often been associated with disordered or hierarchical pore structures. Theoretical studies suggest that catalysts with hierarchical pore structure exhibited higher catalytic activity allowing easy diffusion of reactants and products.

Fig. 8 shows different types of pores that can exist in a porous solid. Pore ranging from open, closed, inkbottle pores, interconnected pores, micropores (< 2 nm), mesopores (2-50 nm), macropores (> 50 nm) and interparticle voids.

At low relative pressures (P/P_o) monolayer and multilayer adsorption takes place in the pores of adsorbate until capillary pore condensation of adsorptive (N_2) starts. On reaching critical multilayer adsorption thickness, hysteresis originates due to the onset of capillary pore condensation of adsorptive gas. As shown in fig.9, for those C-TiO_2 samples which were calcined at 300^o C, a relative increase in N_2 quantity adsorbed at low P/P_o (< 0.2) has been observed, which could be due to micropore filling (presence of micropores). As the calcination temperatures of 10 wt% and 30 wt

% Carbon- TiO_2 extrudates increases from 300° C to 500° C, capillary pore condensation happens at higher (P/P_o) indicating the presence of larger pores.

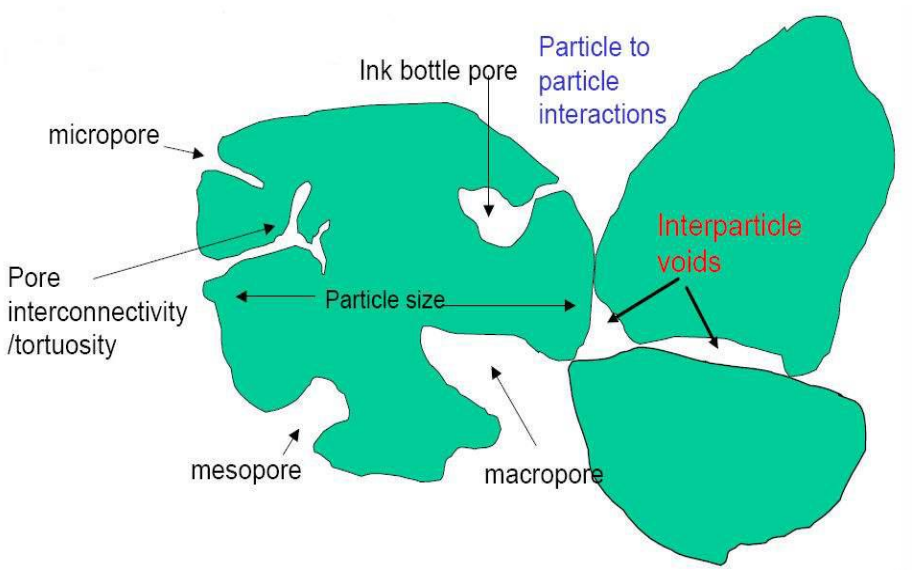

Fig.8 Pore size classification (micropores, mesopores, inkbottle pores, interparticle voids etc.) (Ref. 39)

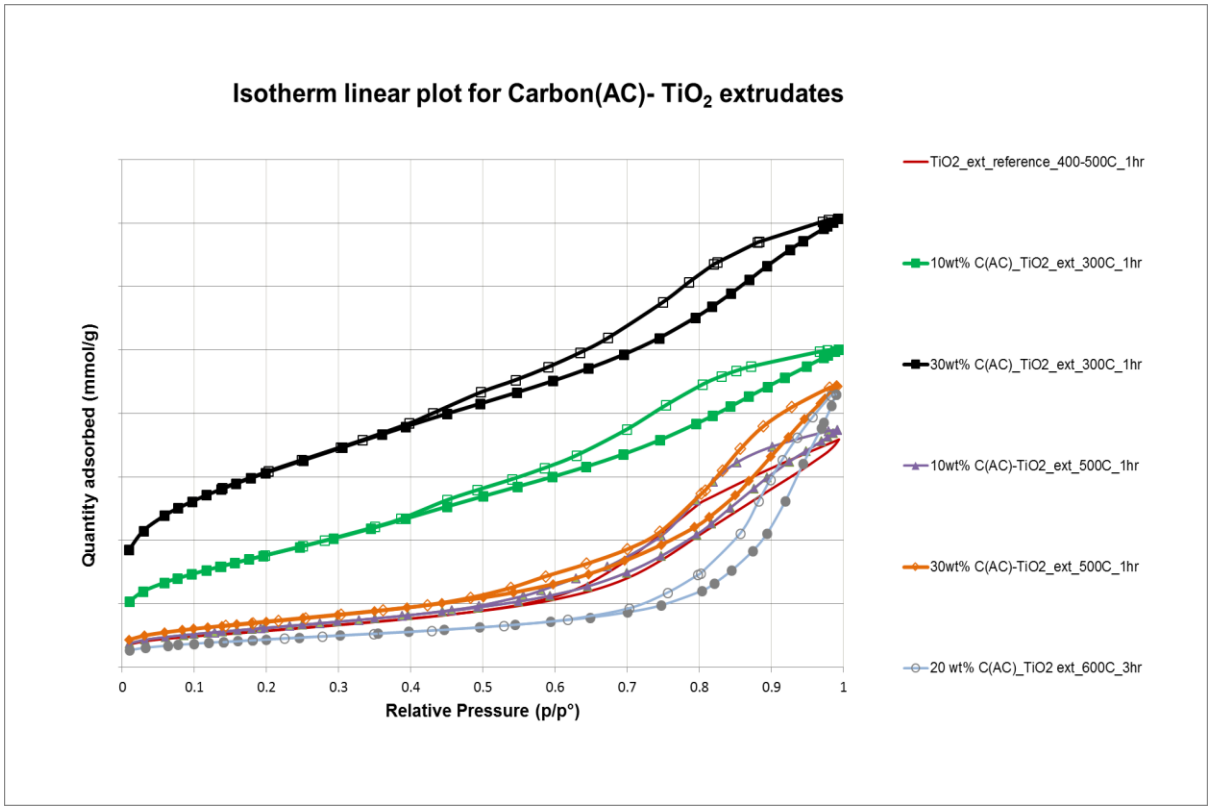

Fig. 9 Isotherm linear plot of different Carbon (AC)-TiO_2 composite supports calcined at different temperature

The width of the H2 type hysteresis loop can be directly correlated to the presence of complex pore structure (hierarchy of pores or ink bottle type pores exist). The delayed condensation of adsorbate over wide range of P/ P_o in case of 10 wt% and 30 wt % Carbon- TiO_2 extrudates calcined at 300 ^oC can be due to pore network effect. During the adsorption in ink bottle pore network, capillary pore condensation in small pores occurs first, which reduce the barriers for capillary condensation of interconnected larger pores of the network due to spillage of condensate to neighboring pores[38]. Therefore complete condensation within a pore network happens gradually (delayed condensation) from small to large pores. This explains the shape of adsorption hysteresis in case of samples calcined at 300 ^oC (fig.9).

The evaporation of capillary condensed liquid during desorption from ink bottle pore networks depends upon desorption from the narrow neck of pore. In other words desorption from pore body depends on size of neck and connectivity of pores. The relative pressure at which condensate from neck desorbs initiates desorption from blocked pores, which is responsible for characteristic desorption hysteresis.

The physisorption isotherm can be transformed to obtain a BET linear plot, from which monolayer adsorbed quantity can be derived which form basis for calculation of surface area. BET surface area, t-plot micropore surface area, BJH desorption pore volume analysis of Activated Carbon (AC)-TiO_2 extrudates calcined at different temperatures are listed in Table.2. It is evident that as the carbon loading increases from 10 wt% to 30 wt% there is significant increase in surface area and pore volume among the samples calcined at 300°C. This could be due to retainment of carbon content in the samples even after calcination. Whereas for those samples calcined at 500°C there is only slight increase in surface area and pore volume indicating that carbon might have combusted completely (leaving voids) or very little carbon content is remaining. But there is decrease in surface area for 20 wt % C(AC) -TiO_2 calcined at 600°C/3hr which could be due to transformation of anatase to rutile phase[40].

Sample (Activated Carbon AC + TiO_2)	BET surface area (m2/g)	t-plot micropore area (m^2/g)	Pore volume (cm3/g)
TiO_2 reference ext_450-500°C/1hr	80-95	N/A*	0.2-0.25
10 wt.% C(AC)-TiO_2 ext_300°C/1hr	288	N/A	0.34
30 wt.% C(AC)-TiO_2 ext_300°C/1hr	495	64	0.42
10 wt.% C(AC)-TiO_2_ext_500°C/1hr	101	N/A	0.26
30 wt.% C(AC)-TiO_2_ext_500°C/1hr	117	1	0.31
20 wt. % C(AC)-TiO_2_ext_600°C/3hr	72	2	0.30

Table 2. BET surface area and pore volume analysis of Activated Carbon (AC)-TiO2 composites

BJH desorption pore size distribution plots of C(AC)-TiO_2 composite extrudates are shown in fig.10. As the calcination temperature increases, pore width peak shifts towards right with peaks getting broader. For 10 wt% and 30 wt % C(AC) -TiO_2 calcined at 300°C the peak at 30 Å could be attributed to micropores and pores arising due to removal of water molecules. This peak can be referred to as pseudo peak because of inability of N_2 adsorptive to probe micropores (<2 nm). For samples calcined at 500°C, there exist pores over broad range of pore sizes (50-200 Å) confirming the presence of hierarchical pore structure.

These pores could be a combination of mesopores, large ink bottle pores and branched pore networks formed upon burning carbon content in the samples during calcination. BJH pore size analysis using modified kelvin equation considered to underestimate pore size analysis of pores less than 10 nm size by 20-30 %[39].

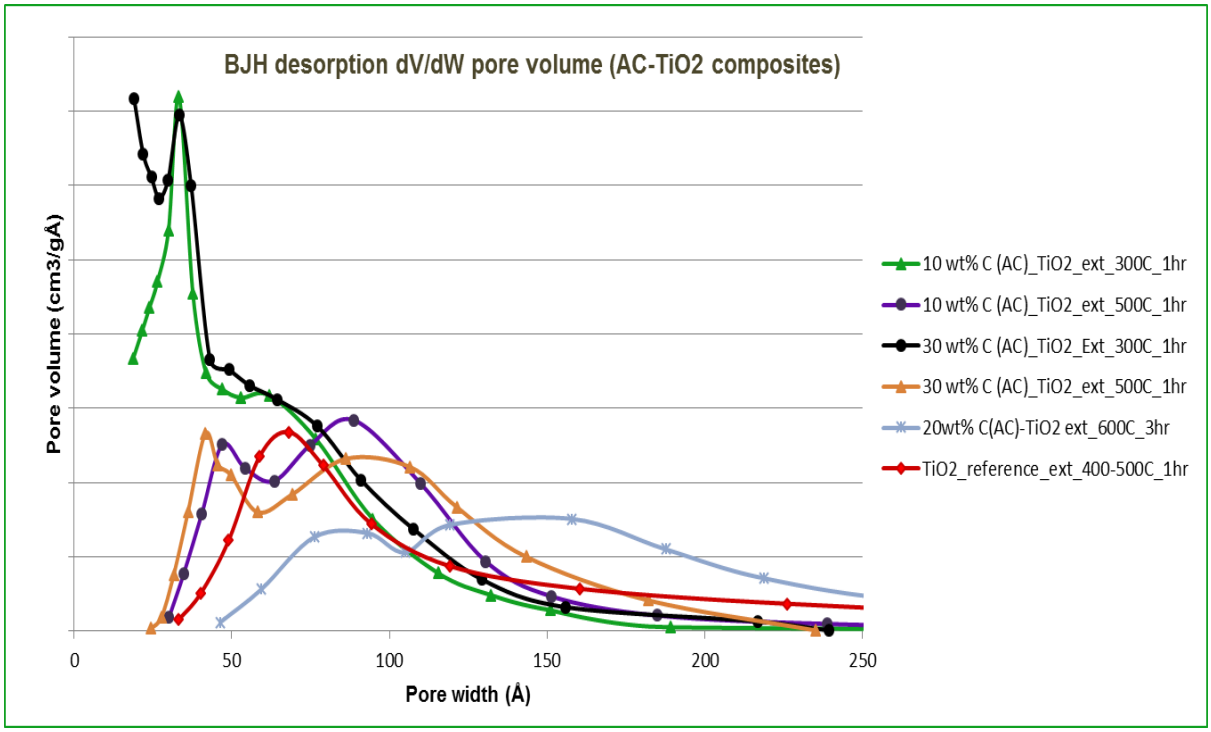

Fig.10 BJH desorption pore size analysis of 10 wt% and 30 wt% Activated Carbon (AC)-TiO_2 extrudates calcined at different temperatures

In case of samples calcined at 300°C both carbon and TiO_2 are present in the sample. When N2 at 77K is used as adsorptive, due to its quadrapole moment it exhibits specific interactions with the surface hydroxyl groups and exposed ions of the TiO_2. As Carbon is neutral, N_2 doesn't have any such interaction with carbon. If both carbon and TiO_2 are present in a same sample N_2 prefers to adsorb on TiO_2 surface over Carbon. Therefore pore size distribution of such samples using N_2 as adsorptive does not accurately estimate the contribution due to carbon. The same is reflected in pore size distribution plots of 10 wt% and 30 wt % C(AC) -TiO_2 calcined at 300°C (pseudo peak). Meanwhile quenched solid density functional theory (QSDFT) and molecular simulations can be used to accurately estimate pore size distribution and adsorption isotherms of porous carbons-TiO_2 supports. QSDFT takes into account surface heterogeneity of samples as well[42].

3.1.2. **Carbon (GC) -TiO_2 extrudes**:

Fig.11 shows isotherm linear plot of different Carbon (GC)-TiO2 composites respectively. Adsorption and desorption curves of all the samples show a hysteresis which belong to type IV isotherm (characteristic of mesoporous materials). Hysteresis curve has been identified as H3 type for samples calcined at 300^{o}C which is typical for slit shaped pores (ordered open ended pores) because there is no limiting adsorption at high relative pressures. This type pores can increase the kinetics or diffusion of reactants/products through the pore structure. The explanation of isotherm plots and BJH pore size distribution plots for Carbon-TiO_2 supports which has been given in the previous section is applicable for all types of carbons used for preparing composites. Therefore explanation for plots with similar trends in isotherms and pore size distribution plots will not be discussed again.

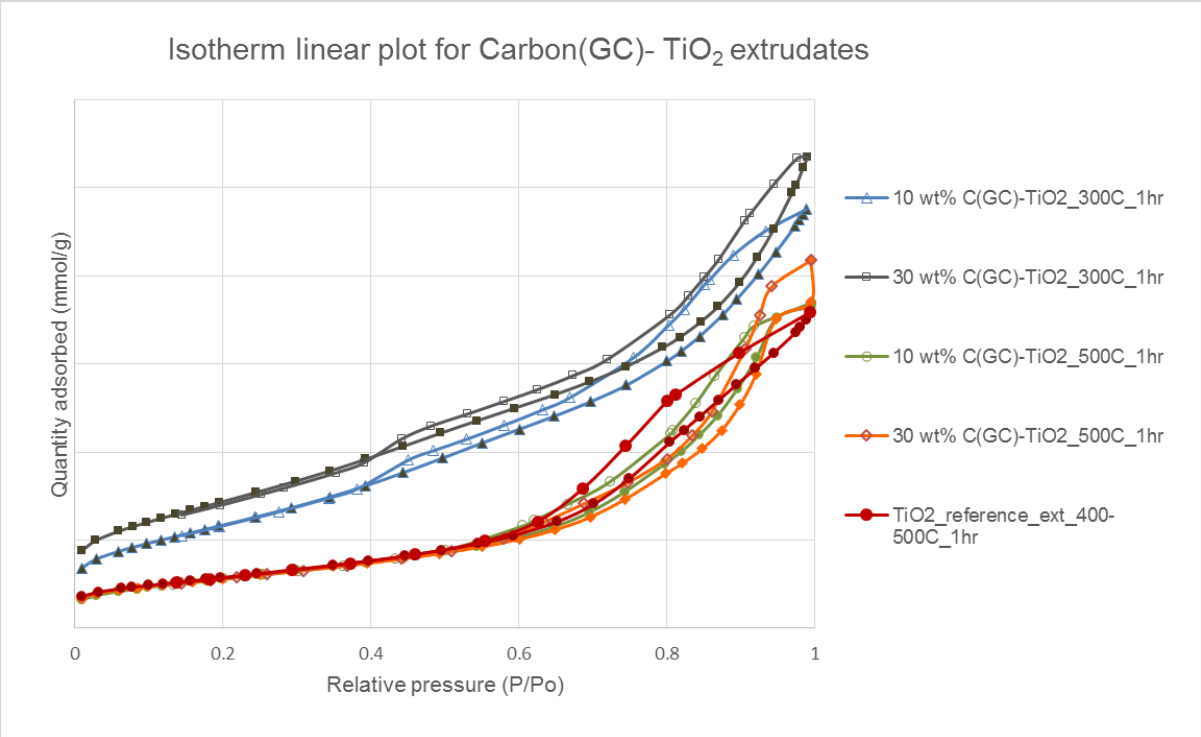

Fig. 11 Isotherm linear plot of different Carbon (GC)-TiO2 composites calcined at different temperature.

Sample (Graphite carbon GC +TiO_2)	BET surface area (m2/g)	t-plot micropore area (m^2/g)	Pore vol. (cm3/g)
TiO_2 reference ext_450-500°C/1hr	80-95	N/A*	0.20-0.25
10 wt.% C(GC)-TiO_2 ext_300°C/1hr	192		0.33
30 wt.% C(GC)-TiO_2 ext_300°C/1hr	233		0.36
10 wt.% C(GC)-TiO_2_ext_500°C/1hr	92		0.26
30 wt.% C(GC)-TiO_2_ext_500°C/1hr	92		0.29
20 wt. % C(GC)-TiO_2_ext_600°C/3hr	61		0.32

Table.3 BET surface area and pore volume analysis of Carbon (GC)-TiO_2 composites

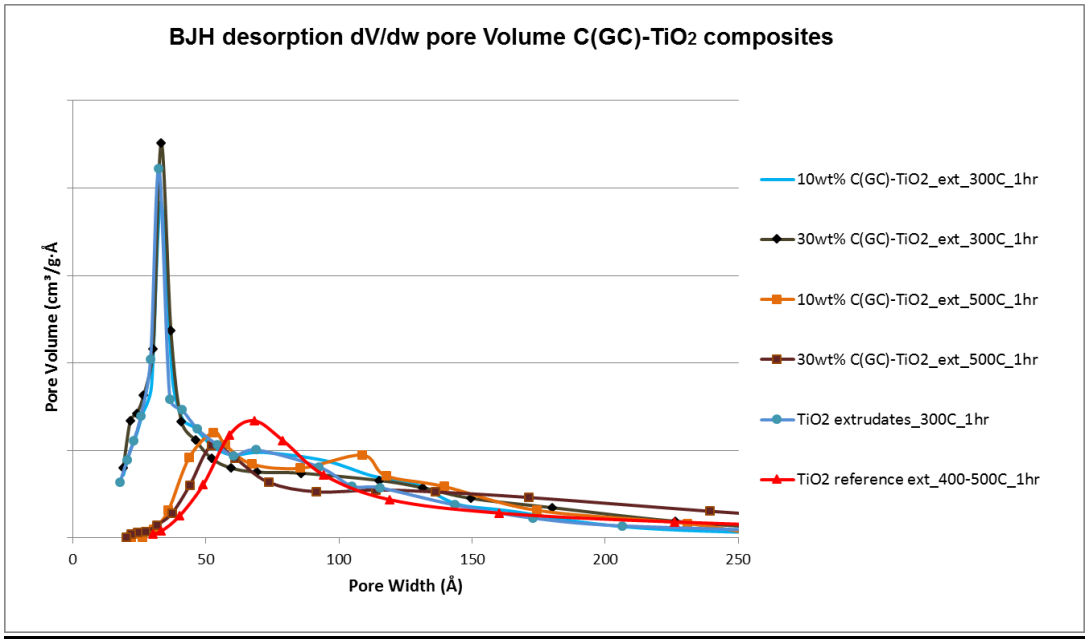

Fig.12 BJH desorption pore size analysis of 10 wt% and 30 wt% Carbon (GC)-TiO_2 extrudates

3.2. Carbon-Alumina composite supports

a) Activated carbon (AC)- Al_2O_3 supports:

For Activated carbon (AC)-Al_2O_3 composite supports there exists no significant change in surface area and pore size distribution with increasing carbon loadings and calcination temperatures. This could be due to sintering of alumina particles at high temperatures which collapses pores formed due to carbon combustion. Isotherm is of type IV and hysteresis is type H1 indicating presence of narrow cylindrical pores.

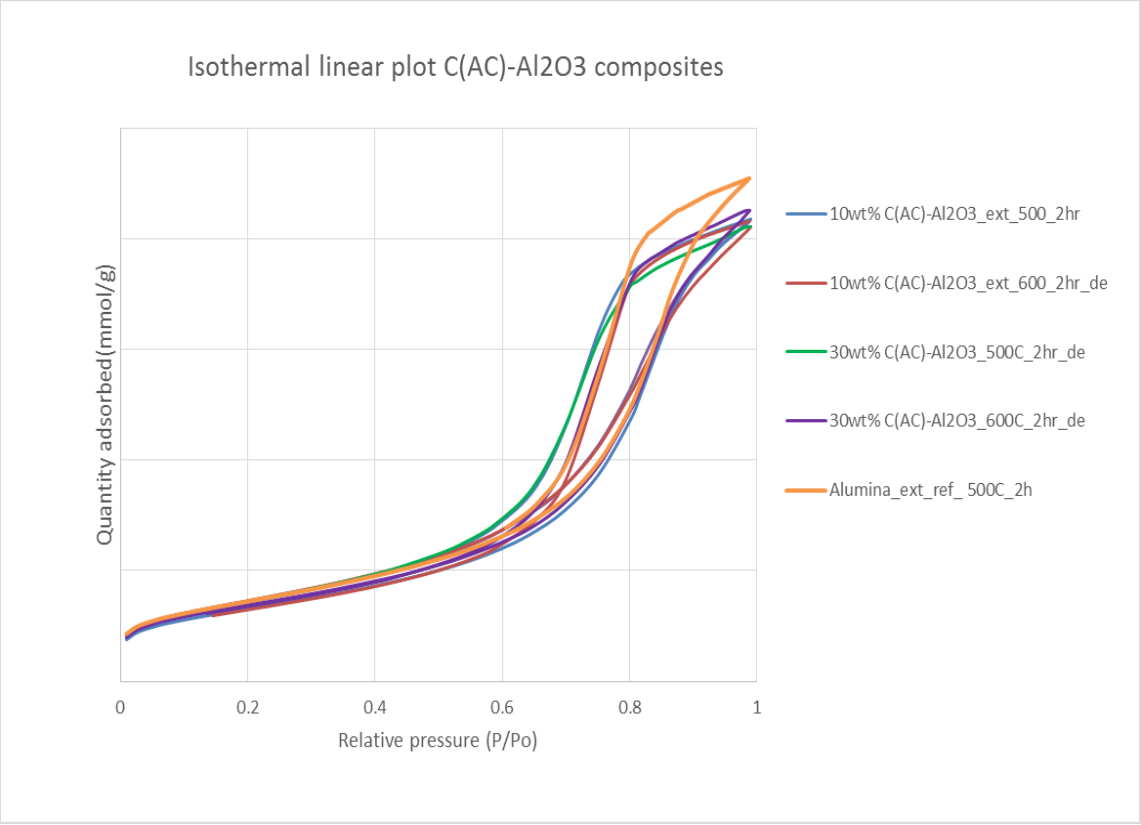

Fig. 13 Isotherm linear plot of different Carbon (AC)-Al_2O_3 composites calcined at different temperatures.

Table.4 BET surface area and pore volume analysis of Carbon (AC)-Al_2O_3 composites

Sample (Carbon (AC) + Alumina)	BET surface area (m2/g)	t-plot micropore area	Pore Vol. (cm3/g)
Alumina_reference_450-500_2hr	280-305	N/A	0.75-0.90
10 wt% C(AC)-Al_2O_3_extrudate_500C_2hr	292	N/A	0.73
30 wt% C(AC)-Al_2O_3_extrudate_500C_2hr	295	N/A	0.72
10 wt% C(AC)-Al_2O_3_extrudate_600C_2hr	266	N/A	0.73
30 wt% C(AC)-Al_2O_3 _extrudate_600C_2hr	279	N/A	0.74

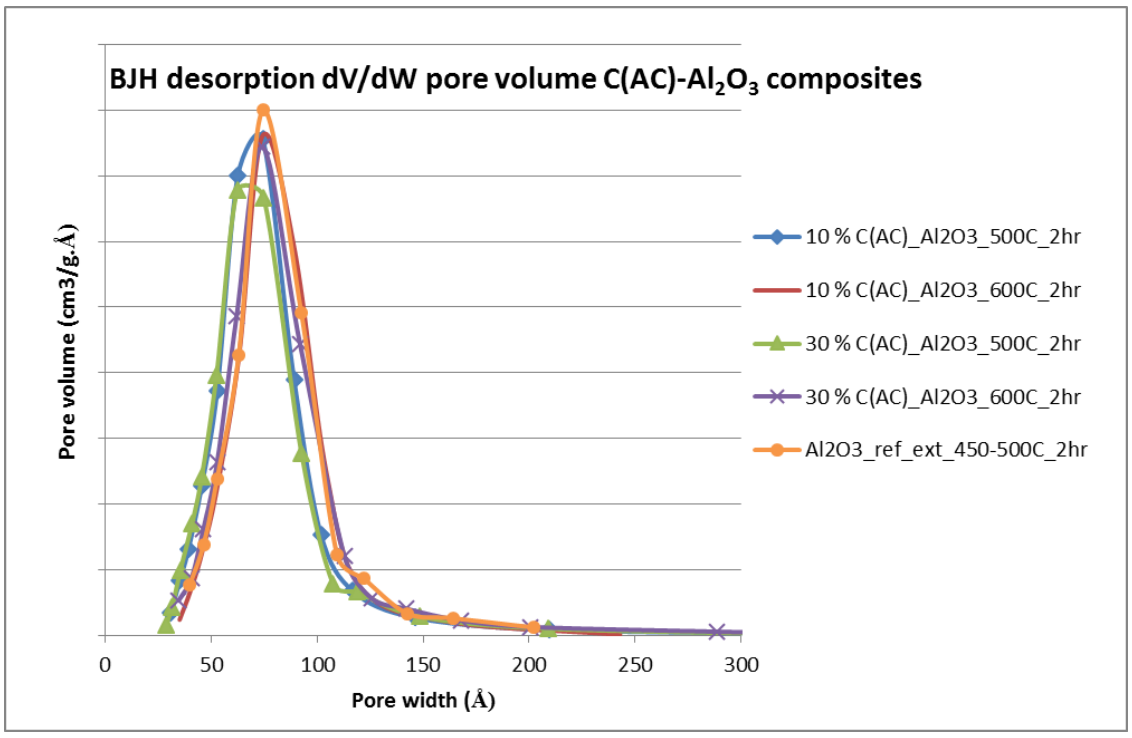

Fig.14 BJH desorption pore size analysis of 10 wt% and 30 wt% Carbon (AC)-Al_2O_3 extrudates

b) Carbon black (CB)-Al_2O_3 extrudes:

Using this 20wt% and 40 wt% C(CB)-Al_2O_3 extrudates were prepared and calcined at 500^o C and 600^o C.

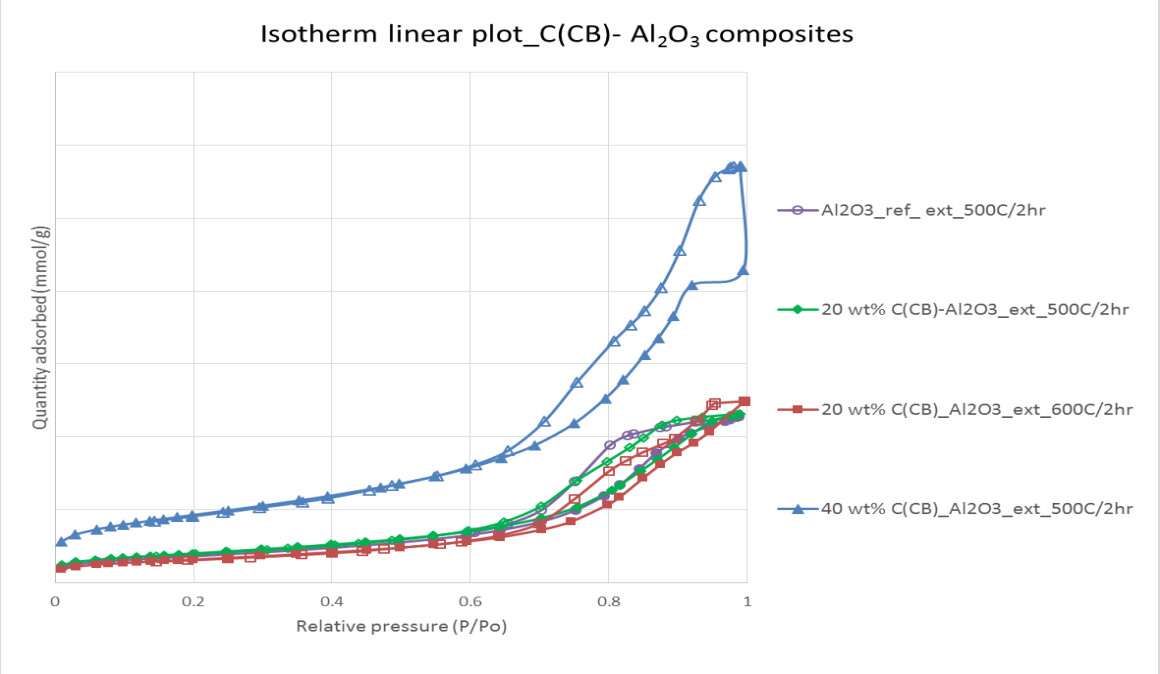

Fig. 15 Isotherm linear plot of 20 wt% and 40 wt% Carbon black (CB)-Al_2O_3 extrudates calcined at different temperatures.

As shown in fig.15 at low (20 wt%) carbon black loadings the isotherm plot remains same, indicating that carbon black particles might be present on the surface of Alumina particles. Whereas at high carbon loadings (40 wt%) carbon black might have penetrated inside the alumina particles and on combustion results in voids left by burning chained carbon black particles. This is reflected in case of 40 wt% C(CB)_Al_2O_3 extrudates calcined at 500^{o}C isotherm plot. It shows a sudden rise of capillary adsorption at high relative pressures and as a small hump at 200 Å in BJH pore size distribution (presence of large mesopores due carbon combustion). Whereas for those samples calcined at 600^{o}C no change in isotherm plots can be attributed to collapse of pores due to sintering of alumina particles.

Sample (Carbon black CB +Al_2O_3)	BET surface area (m2/g)	t-plot micropore area (m^2/g)	Pore vol. (cm3/g)
Al_2O_3 reference ext_450-500°C/2hr	280-305	N/A	0.75-0.90
20 wt.% C(CB)- Al_2O_3 ext_500°C/2hr	323	24	0.81
40 wt.% C(CB)- Al_2O_3 ext_500°C/2hr	373	39	0.98
20 wt.% C(CB)- Al_2O_3 _ext_600°C/2hr	256	11	0.86

Table.5 BET surface area and pore volume analysis of Carbon black (CB)-Al_2O_3 composites

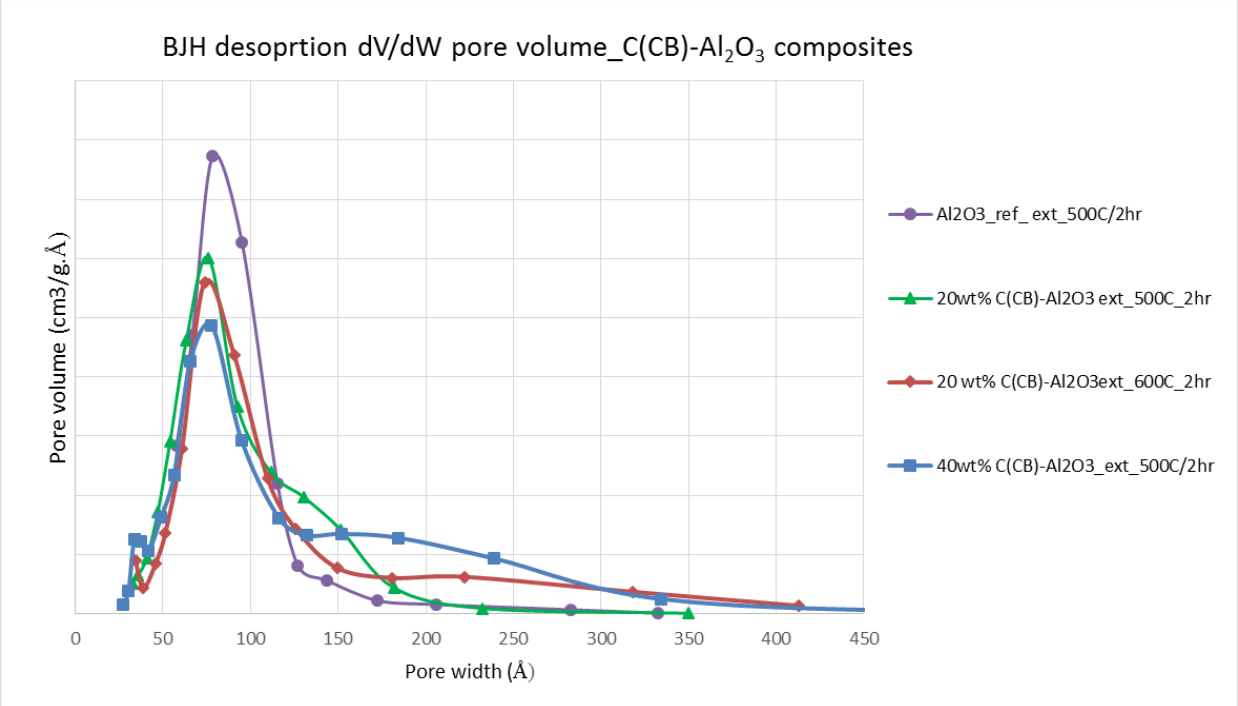

Fig.16 BJH desorption pore size analysis of 20 wt% and 40 wt% Carbon black (CB)-Al_2O_3 extrudates calcined at 500 °C and 600 °C.

3.2 PZC measurements:

PZC measurements of Carbon (AC) –TiO_2 samples are shown in table 6. It implies that presence of carbon in samples decreased the acidity of the TiO_2 supports. For samples calcined at 300^{o}C the PZC is in range 6 -7.5 and the pH of impregnated vanadate precursor solution is between1-2 (i.e, pH< PZC). Therefore the surface of supports will be more positively charged and are capable of anchoring anionic vanadate complexes strongly on the support.

Sample (Carbon-TiO_2 composites)	pH at PZC
10 wt.% C(AC)-TiO_2 ext_300°C/1hr	6-7
30 wt.% C(AC)-TiO_2 ext_300°C/1hr	7-7.5
10 wt.% C(AC)-TiO_2_ext_500°C/1hr	4-5
30 wt.% C(AC)-TiO_2_ext_500°C/1hr	5-5.5

Table.6 PZC measurements of Carbon (AC)-TiO2 composite supports.

The PZC of Activated carbon (8-10), Graphitic carbon (4-5) and carbon black (8-10)[5].

3.3 SEM analysis:

SEM images of V_2O_5/30wt%-C(AC)-TiO_2_500^{o}C extrudates in increasing order of magnification from a) to d) are shown in fig 17. It has been observed that cabon-TiO_2 samples calcined at 500^{o}C has irregular pore structures formed upon combustion of carbon and this is in agreement with the wide pore size distribution curves in fig.10. There exists non-uniform distribution of V_2O_5 on the supports which can be seen in c) and d). This implies that coverage of V_2O_5 could be more than monolayer which could decrease the number of active sites available for the reaction thereby decreasing catalytic activity.

Whereas SEM images of V_2O_5/30wt%-C(AC)-TiO_2_300^{o}C extrudates as shown in fig 18 (e to h). There are no visible pores in µm-range but there exists lot of micropores due to carbon contentas confirmed from textural properties. From this we can infer that Activated carbon present in these supports is mixed well with the TiO_2 precursors during mulling process. V_2O_5 seems to be uniformly distributed on C-TiO_2 supports.

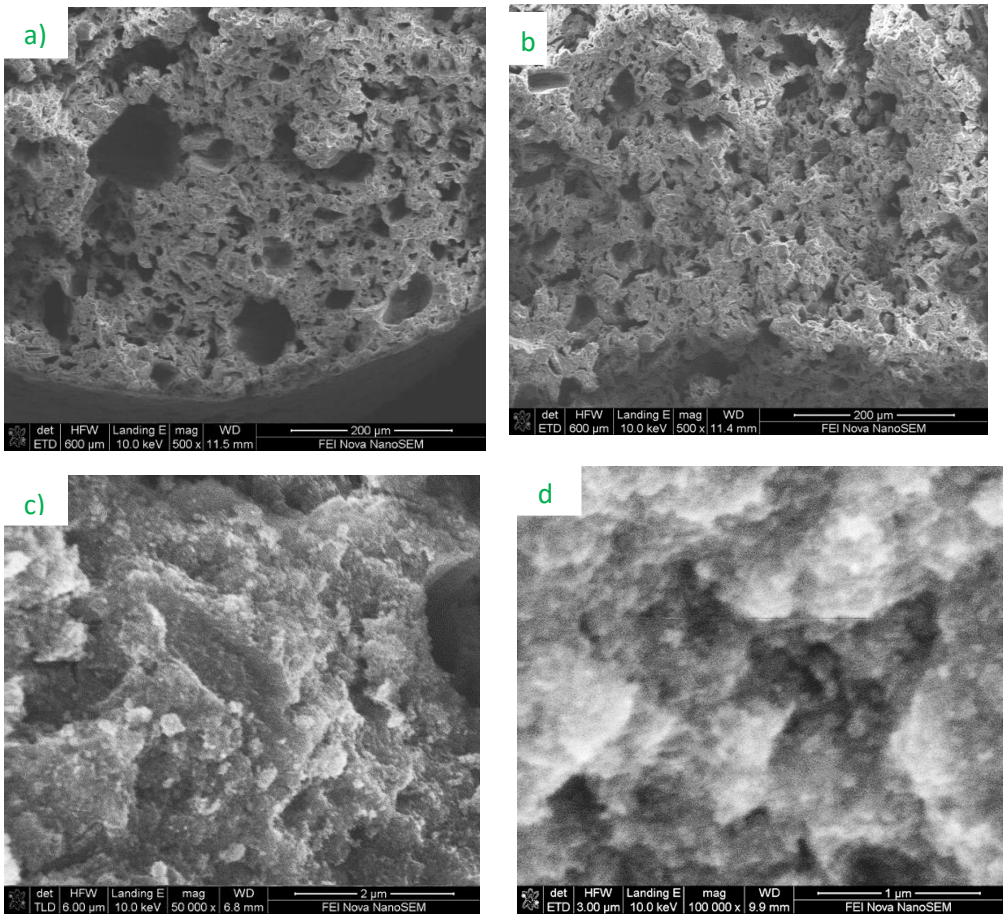

Fig17: SEM images of V_2O_5/30wt%- C(AC)-TiO_2/500^oC extrudates in increasing order of magnification from a) to d).

Based on SEM and PZC measurements it has been confirmed that V_2O_5 dispersed on carbon as well. Since uniform monolayer distribution of V_2O_5 is needed for achieving high catalytic activity, the supports calcined at 300^oC could result in higher catalytic activity than the supports calcined at 500^oC.

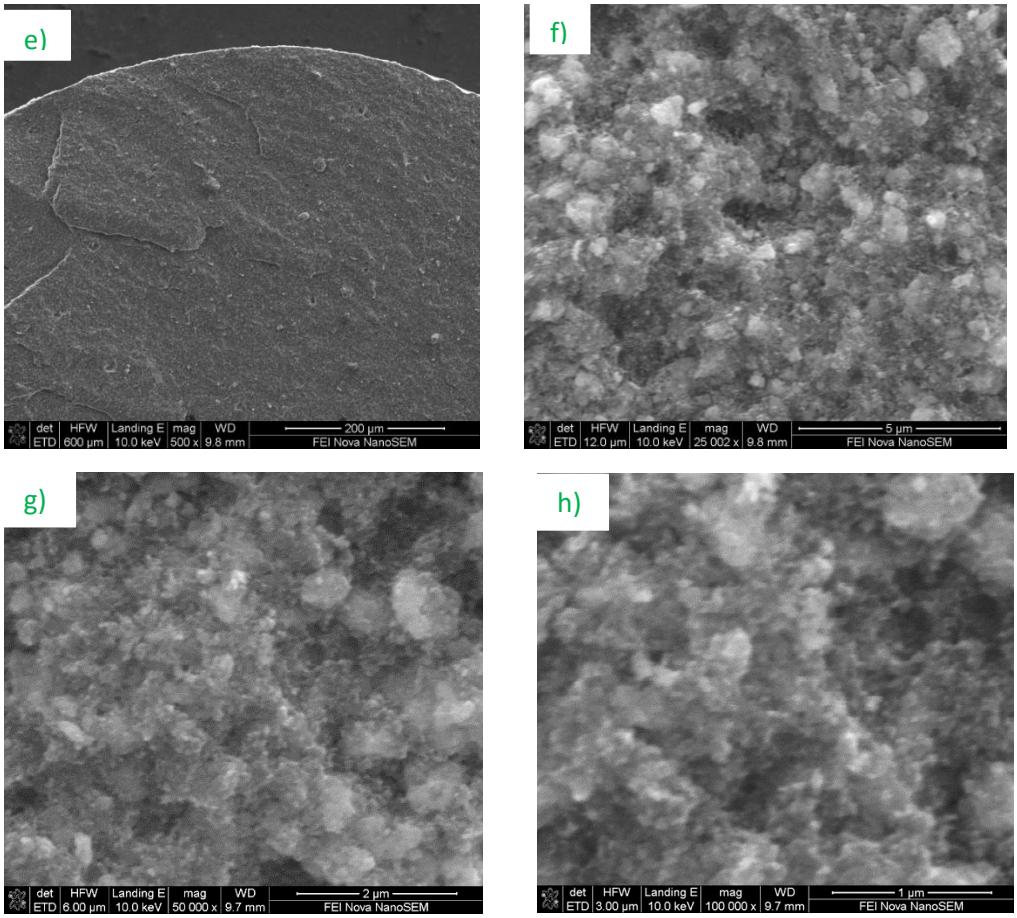

Fig 18: SEM images of V_2O_5/30wt%- C (AC)-TiO_2_300^oC extrudates in increasing order of magnification from e) to h).

3.4 DeNOx activity testing results:

The catalytic activity testing for V_2O_5/10-30 wt% Carbon (AC, GC) + TiO_2 catalysts have been carried out for low temperature NOx reduction using NH_3 as a reducing agent. The relative activity (% NO conversion) of all the samples compared to reference catalyst has been listed in table.6 below.

The percentage NOx conversion ($DeNO_x$) is defined as follows:

$$\%\ NO\ conversion = \left(\frac{NO(in) - NO(out)}{NO(in)}\right) * 100\ \%$$

S.NO	Sample description V_2O_5 supported (Carbon + TiO_2) composites	Relative Activity (% NO conversion) without water at 150 ^{0} C	
		Activated Carbon (AC) loading	Graphitic carbon (GC) loading
1	Reference catalyst	100	100
2	x wt% V_2O_5/10 wt.% Carbon - TiO_2 ext_300°C	157	-
3	x wt% V_2O_5/10 wt.% Carbon - TiO_2 ext_500°C	88	98.4
4	x wt% V_2O_5/ 30 wt.% Carbon- TiO_2_ext_300°C	169.9	180.8
5	x wt% V_2O_5/ 30 wt.% Carbon- TiO_2_ext_500°C	86	-
6	y wt% V_2O_5/ 20 wt.% Carbon- TiO_2_ext_600°C	70	65

Table.7. Relative activity (% NO conversion) of x (1-5) wt% V_2O_5 /10-30 wt% Carbon (AC, GC) + TiO_2 catalysts compared to reference catalyst

Observations

As shown in the table, the relative activity of x wt% V_2O_5/ (10 & 30 wt%) Carbon (AC, GC) + TiO_2 catalysts calcined at 300^o C shows significant higher % NO reduction (> 50 % increase in activity) than the reference catalyst (in absence of moisture). Whereas for those samples which were calcined at 500^o C and 600^o C the relative activity (% NO reduction) decreases. Activity testing have also been carried out in the presence of 8-12 vol% H_2O in same flue gas composition (the results of which are not included here). The activity of the samples calcined at 500^o C and 600^o C in presence

of 8-12 vol % H_2O were consistent with the results without H_2O. On the contrary, there is an immediate decrease in the catalytic activity (% NO reduction < 30) on Carbon-TiO_2 supports calcined at 300 ^{o}C when H_2O is added.

Discussion

From the testing results, retaining Carbon content in TiO_2 supports enhanced the catalytic activity of NO reduction (in the absence of H_2O) but decreased the activity in presence of 8-12 vol % H_2O. There can be multiple hypothesis to explain the above results-

a) Presence of porous carbon content in TiO_2 supports enhance the diffusion of reactants (NO, NH_3) and products (N_2) through the porous structure thereby showing significant increase in the catalytic activity in the absence of H_2O. When H_2O is present, catalysts get deactivated due to blockage of micropores of carbon by condensation of H_2O[45]. The deactivation rate has been increased by increasing H_2O concentration in the flue gas. This could be due to competitive absorption of H_2O on the active sites which are meant for NH_3 absorption.

b) Adding porous carbons along with TiO_2 precursors during mulling and extrusion improve peptization by separating TiO_2 particles with carbon. This is in agreement with Carbon-TiO_2 supports calcined at 300^{o}C having higher surface area than reference supports. These high surface area porous C-TiO_2 support can ultimately produce highly dispersed active phase (V_2O_5) on the support exposing more active sites for the reaction to occur.

c) The surface functional groups present on porous carbons might also have contributed for the catalytic activity. The PZC of the C-TiO2 supports are in the range of 6.5 -7.5. Thus making these sites capable of anchoring of active metal complexes (vanadium oxalate solution pH 1-2) during impregnation. Thereby extending the dispersion of V_2O_5 onto the carbon surface. Alternatively acidic surface groups on porous carbons can itself act as catalysts by adsorbing NH_3 and NO and allowing the reaction to proceed.

All the above factors could act synergistically to result in high catalytic activity.

Possible mechanism

Many papers proposed different reaction mechanisms for NH_3-SCR reaction on V_2O_5 supported TiO_2 catalysts. Based on various spectroscopic and in-situ characterization techniques variety of intermediates have been identified. However, these experimental data are far from real industrial working conditions in the absence of SO_x, H_2O. Therefore proposing a reaction mechanism under real working conditions is still a challenge. Many authors agree the following reaction mechanism (amide-nitrosamide mechanism) on V_2O_5-TiO_2 catalysts[33].

The amide-nitrosamide mechanism is based on Eley- Rideal reaction mechanism as shown in Fig.19. In which NH_3 is first adsorbed over Lewis acid sites of active metals (V_2O_5). The adsorbed NH_3 gets activated and reacts with gas phase NO resulting in formation of nitrosamide intermediate. This intermediate then decomposes to N_2 and H_2O. The reaction is essentially a coupling reaction between adsorbed NH_3 and NO. Therefore use of NH_3 as reducing agent can result in high N_2 selectivity, as one atom of N in N_2 product comes from NH_3 and other from NO.

The mechanism is of redox type, where adsorption and activation of NH_3 results in reduction of V^{5+} to V^{4+} species. After subsequent reaction with gas phase NO (to give N_2, H_2O) the catalyst is left reduced form (V^{4+} -OH). The reduced V^{4+} gets re-oxidized to V^{5+} species from gaseous oxygen, thus regenerating the catalyst active site.

In our present case with Carbon-TiO_2 supported V_2O_5 catalysts. The acidic surface functional groups (carboxyl and hydroxyl groups) on porous carbons could have contributed to the catalytic activity. Catalytic activity can be directly related to presence of oxygen containing functional groups on the porous carbon surface.

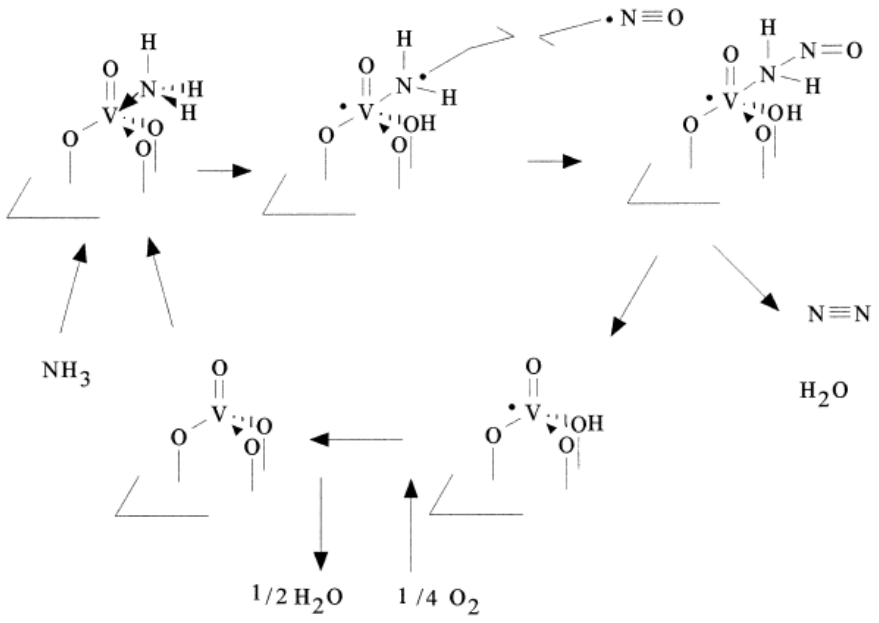

Fig.19 Mechanism NO reduction by NH_3-SCR reaction on supported V_2O_5 catalysts (Ref. 43)

These surface oxygen groups of porous carbons can decompose to CO and CO_2 at different temperature ranges. The carboxylic acids groups release CO_2 at low temperatures (100-450º C), anhydrides release CO+CO_2 at temperatures (350-600 º C), lactones and phenols release CO at (500-800 º C) and carbonyl decompose to release CO at high temperatures (650-950 º C)[44]. Therefore at operating temperatures of 150 º C most of the oxygen containing functional groups on carbon surface are stable and can contribute to the low temperature NO_x reduction activity. Teng et al. proposed a mechanism for low temperature NO_x reduction using NH_3 on carbon catalysts[45] as shown in fig.20. In which NH_3 first adsorbs on phenolic hydroxyl groups resulting in the formation of $CO^-(NH_4^+)$ complex on carbon surface, whereas NO interacts with neighboring carbonyl or adsorbed oxygen species to form C(ONO) complexes as shown in fig.19 . These two complexes then react on the surface and release N_2 and H_2O (Langmuir-Hinshelwood type mechanism). The reduced carbon surface functional groups can be can re-oxidised in presence gaseous oxygen thus completing the catalytic cycle.

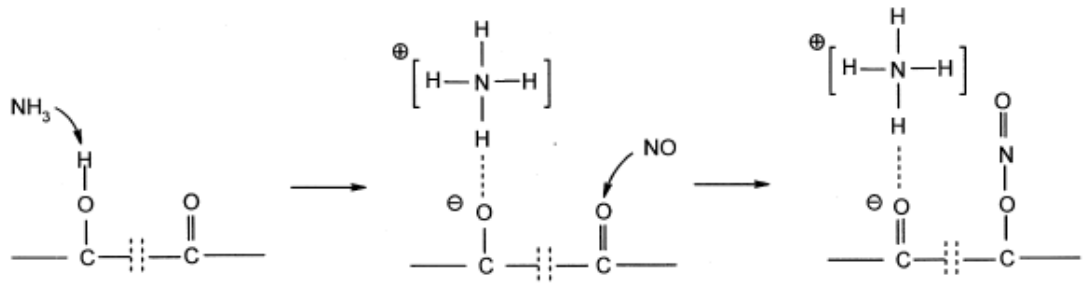

Fig.20 Reaction scheme of formation of surface intermediates during NO reduction on carbon catalysts (Ref. 45)

Thus using porous carbons not only act as support but also helps in increasing the low temperature NOx reduction activity of V_2O_5-TiO_2 catalysts.

3.5 Hydroprocessing activity testing results:

The HDS and HDN activity of Carbon-Al_2O_3 composite supported NiMO catalysts were measured in terms of average temperature required (avg.T_{req}) to achieve certain conversion rate over a period of time. The avg.T_{req} HDS has been measured for achieving a constant conversion of S-containing impurities. The avg.T_{req} HDN has been measured for achieving a constant conversion of N-containing impurities. Table.7 shows the relative difference in avg.T_{req} HDS and HDN of different NiMO supported on C-Al_2O_3 composites compared to reference reference catalysts to achieve desired conversion rate. All the catalysts show a positive difference in avg. T_{req}, which refers that more temperature equal to difference value (compared to T_{req} for reference catalyst) is needed to achieve desired conversion rates.

20 wt% & 40 wt% Carbon black (CB)-Al_2O_3_500^oC catalysts show activity comparable to that of reference catalyst (delta avg. T_{req}= 2 approx.). This could be complemented with presence of hierarchical pores over wide range (90-350 Å) in pore size distribution plots thus allowing larger impurity molecules to pass through the pores. The catalytic activity decreases as the calcination temperature increases, and this decrease is more pronounced in HDN activity. This could be due to poor dispersion of active phase thus reducing the active sites available for the reaction.

Samples (with NiMO catalysts)	delta avg. T_{req} HDS (relative to reference)*	delta avg. T_{req} HDN (relative to reference)*
20 wt% C(CB)-Al_2O_3_ext_500^oC/2hr	2.1	2.3
20 wt% C(CB)-Al_2O_3_ext_600^oC/2hr	3.3	6
40 wt% C(CB)-Al_2O_3_ext_500^oC/2hr	2.4	5
40 wt% C(CB)-Al_2O_3_ext_600^oC/2hr	6.2	14.8
10 wt% C(AC)-Al_2O_3_ext_500^oC/2hr	8	11.9
30 wt% C(AC)-Al_2O_3_ext_500^oC/2hr	9	31
30 wt% C(AC)-Al_2O_3_ext_600^oC/2hr	10	15.1

Table. 8 Relative avg. T_{req} for HDS and HDN of NiMO supported Carbon-alumina composites.

Whereas catalysts on activated carbon C(AC)- Al_2O_3 composites show poor catalytic activity since they show large difference in avg. $T_{req.}$ The textural properties of all C(AC)- Al_2O_3 composites show negligible difference compared to reference supports but the activity is much lower compared to reference catalyst which again could be due to sintering of active phase (NiMOS) into large crystals. These results are in disagreement with those of reported by Shaoping Xu et.al, where they proposed that NiMO on alumina-activated carbon composites increased catalytic activity of DBT compared to pure alumina and activated carbon as supports[24].

Conclusion

It can be concluded that porous carbons can be best additive to TiO_2 for improving textural properties of the supports. Using different types of carbon and controlling quantity of addition of carbon sources, pore structure of TiO_2 can be tuned to yield high surface area supports with hierarchical pore structures. Using these tuned supports for impregnation of active metals (V_2O_5) on the supports (TiO_2) would improve dispersion of active metals. Thereby exposing more number of catalytically active sites for the reaction to proceed and hence increase the NO reduction activity in absence of water in feed composition. Catalyst deactivation mechanisms known to occur in NO reduction using NH_3 predominate when water is added to feed thereby nullifying the advantages achieved in active phase dispersion in C-TiO_2 composites.

In activated carbon-alumina composite supports pore structure modification does not occur and other properties such as acidity of the supports, molybdenum slab dispersion, and surface structure play a major role in catalytic activity. The composites used as supports showed relative lower activity in VGO hydrotreating compared to alumina supports. NOx catalytic activity.

Outlook

Surface functional groups on porous carbons can be tuned by various methods in order to increase their contribution in improving catalytic activity of carbon-metal oxide composite supports. Oxygenated functional groups on carbon surface can be increased by various post-treatment methods like oxidizing using nitric acid (HNO_3) or by oxidation in diluted oxygen (5 vol%) at temperatures 350-450 ^oC[46]. Pretreated porous carbon surfaces can anchor more active metal complexes ultimately increasing the dispersion of active metals onto carbon surfaces and hence increase the catalytic activity.

References

1. Nitrogen Oxides (NOx), Why and How They Are Controlled, EPA-456/F-99-006R November 1999 (www3.epa.gov/ttncatc1/dir1/fnoxdoc.pdf)
2. How nitrogen oxides affect the way we live and breathe, US Environmental protection agency, EPA-456/F-98-005 September 1998 (www3.epa.gov/airquality/nitrogenoxides/)
3. J.N. Armor (Ed.), Environmental Catalysis, ACS Symposium Series, vol. 552, American Chemical Society, Washington, 1994.
4. Satterfield, C.N. Heterogeneous catalysis in industrial practice, 2nd ed. Krieger Publishing, Malabar, 1991.
5. Synthesis of solid catalysts, K.P. de Jong, 2009, Wiley
6. Christian Hulteberg, An Introduction to Catalysis lecture, Jan 2016, (retrieved from(http://www.hulteberg.com/learn-more-about-catalysis-a-free-webinar-by-hce/)
7. G.Centi and S. Perathoner; State of the art in the development of catalytic processes for the SCR of NOx into N_2, Past and present in DeNOx catalysis, *Elsevier,* **2007**.
8. Curtin.T, Selective catalytic reduction of NOx. In Environmental Catalysis (V.H. Grassian, ed.) CRC Press LLC: Boca Raton, Fla, USA, pp. 197, 2005
9. G. Busca, G. Centi, L. Marchetti, F. Trifiro, (Chemical and spectroscopic study of the nature of a vanadium oxide monolayer supported on a high-surface-area TiO2 anatase), Langmuir, 1986, 2, 568–577.
10. Zhenping Zhu, Zhenyu Liu, Shoujun Liu, Hongxian Niu; NO reduction with NH3 over an activated carbon-supported vanadium oxide catalysts at low temperatures Applied Catalysis B: Environmental **1999**, 23, 1229-1233.
11. Israel E. Wachs, Goutam Deo, Bert M. Weckhuysen, Amedeo Andreini, Michael A. Vuurman; Selective Catalytic Reduction of NO with NH3 over Supported Vanadia Catalysts; JOURNAL OF CATALYSIS 1996, 161, 211–221.
12. Wen Jing, Qianqian Guoa,, Yaqin Hou, Guoqiang Ma, Xiaojin Han, Zhanggen Huang; Catalytic role of vanadium(V) sulfate on activated carbon for SO2
13. oxidation and NH3-SCR of NO at low temperatures; Catalysis Communications 56 (2014) 23–26

14. Michael D. Amiridis, Israel E Wachs, Goutam Deo, Jih-Mirn Jehng, and Du Soung Kim; Reactivity of V_2O_5 Catalysts for the Selective Catalytic Reduction of NO by NH3: Influence of Vanadia Loading, H2O, and SO2, Journal of Catalysis, **1996,** 161, 247–253.

14. Enrico Tronconi, Alessandra Beretta; The role of inter- and intra-phase mass transfer in the SCR-DeNOx reaction over catalysts of different shapes, Catalysis Today (1999), 52, 249-258.
15. D. Basmadjian, G.N. Fulford, B.I. Parsons, D.S. Montgomery, The control of pore volume and pore size distribution in alumina and silica gels by addition of water soluble organic polymers. Journal of catalysis, 1962, 1, 547-563.
16. Zhanggen Huang, Zhenping Zhu, Zhenyu Liu; Combined effect of H_2O and SO_2 on V_2O_5/AC catalysts for NO reduction with ammonia at lower temperatures, Applied Catalysis B: Environmental, **2002**, 39, 361–368.
17. S. K. Maity, L. Flores, J. Ancheyta, and H. Fukuyama; Carbon-Modified Alumina and Alumina-Carbon-Supported Hydrotreating Catalysts; Ind. Eng. Chem. Res. 2009, 48, 1190–1195.
18. Maria Pia Ruggeri, Isabella Nova, Enrico Tronconi; Experimental and modeling study of the impact of interphase and intraphase diffusional limitations on the DeNOx efficiency of a V-based extruded catalystfor NH3–SCR of Diesel exhausts, Chemical Engineering Journal 207–208 **(2012)** 57–65.
19. Chang S. Hsu, Paul R. Robinson, Current progress in catalysts for Hydrotreating, Practical Advances in Petroleum Processing, (Vol. 1).
20. Properties of catalysts for hydroprocessing of heavy feed(Chapter-3), Catalysts for upgrading heavy petroleum feeds, page 23-41.
21. Manoj kumar, Babul al, Anand singh et.al, Control of mesoporosity in alumina, Indian Journal of Chemical technology, 2001, 8, 157-161.
22. Xinmei Liu, Xiang Li, Zifeng Yan, Facile route to prepare bimodal mesoporous-Al2O3 as support for highly active CoMo-based hydrodesulfurization catalyst; Applied Catalysis B: Environmental, 2012, 121– 122, 50– 56
23. Fang Liu, Shaoping Xu, Yawu Chi, Dongfeng Xue; A novel alumina-activated carbon composite supported NiMo catalyst for hydrodesulfurization of dibenzothiophene, Catalysis Communications 2011, 12, 521–524.

24. Edward Furimsky, Industrial Carbons (chapter.1), Carbon and carbon supported catalysts in Hydroprocessing, RSC Catalysis series, 2008.
25. José Luís Figueiredo, Manuel Fernando R. Pereira, The role of surface chemistry in catalysis with carbons, Catalysis Today, 2010, 150, 2-7.
26. H.P Boehm, Surface oxides on carbon and their analysis: a critical assessment, Carbon, 2002, 40, 145-149.
27. K. Onuma, Preparation of bimodal alumina and other refractory inorganic oxides – suitable supports for hydrotreating catalysts, Preparation of Catalysts IV, 1987, 543-555.
28. Partic Euzen, Pascal Raybaud, Xenophon Krokidis, Alumina (section 4.7.2), Handbook of Porous Solids, Wiley, 2002, vol.3, 1591.
29. Sounak Roy, B. Viswanath, M. S. Hegde, Giridhar Madras; Low-Temperature Selective Catalytic Reduction of NO with NH_3 over $Ti_{0.9}M_{0.1}O_{2-\delta}$ (M = Cr, Mn, Fe, Co, Cu), J. Phys. Chem. C 2008, 112, 6002-6012.
30. Xiang Li, Dezhi Han, Yongqiang Xu, Xinmei Liu, Zifeng Yan; Bimodal mesoporous γ-Al2O3: A promising support for CoMo-based catalyst inhydrodesulfurization of 4,6-DMDBT; Materials Letters 65 (2011) 1765–1767.
31. Sandeep Badogaa, Rajesh V. Sharmaa, Ajay K. Dalaia, John Adjayeb; Synthesis and characterization of mesoporous aluminas with different pore sizes: Application in NiMo supported catalyst for hydrotreating of heavy gas oil; Applied Catalysis A: General 489 (2015) 86–97
32. Stephen Brunauer, P. H. Emmett, Edward Teller; Adsorption of Gases in Multimolecular Layers, J. Am. Chem. Soc., 1938, 60 (2), 309–319.
33. E. P. Barrett, L. G. Joyner, P. P. Halenda, The Determination of Pore Volume and Area Distributions in Porous Substances. I. Computations from Nitrogen Isotherms, Journal of Americal Chem. Soc. 1951, 73, 373
34. B.C. Lippens, J.H. De Boer, Study of pore systems in catalysis: V vs t-method, Journal of Catalysis, 1965, 4, 319-323
35. Sebastian Storck, Helmut Bretinger, Wilhelm F. Maier; Characterization of micro- and mesoporous solids by physisorption methods and pore-size analysis, Applied Catalysis A: General, 1998, 174, 137-146.
36. J. C. Groen, L. A. Peffer, J. Perez-Ramirez; Pore Size Determination in Modified Micro- and Mesoporous Materials. Pitfalls and Limitations in Gas Adsorption Data Analysis, Microporous and Mesoporous. Materials 2003, 60, 1-17.

37. Reporting physisorption data for gas/solid systems with special reference to the determination of Surface Area and Porosity, Pure & Applied Chem., 1985, 57, 603-619.
38. Matthias Thommes, Physical Adsorption Characterization of Nanoporous Materials, Chemie Ingenieur Technik 2010, 82, No. 7, 1059-1071.
39. Jyrki Asukas, MICROMERITICS GEMINI VII OMINAISPINTA-ALAANALYSAATTORIN VALIDOINT, https://www.theseus.fi/bitstream/handle/10024/51592/Asukas_Jyrki.pdf?sequence=1
40. Dorian A. H. Hanaor, Charles C. Sorrell, Review of the anatase to rutile phase transformation, Journal of Materials Science, 2011, 46, 855-874.
41. M. Thommes, Physical Adsorption Characterization of Ordered and Amorphous Mesoporous Materials, in Nanoporous Materials: Science and Engineering (Eds: G. Q. Lu, X. S. Zhao), Imperial College Press, Oxford, 317, 2004.
42. Alexander V. Neimark, Yangzheng Lin, Peter I. Ravikovitch, Matthias Thommes, Quenched solid density functional theory and pore size analysis of micro-mesoporous carbons, Carbon 2009, 47 (7), 1617.
43. Gianguido Ramis, G. Busca, F. Bregani, P. Forzatti; Fourier transform-infrared study of the adsorption and coadsorption of nitric oxide, nitrogen dioxide and ammonia on vanadia-titania and mechanism of selective catalytic reduction, Applied Catalysis, 1990, 259-278.
44. Jos´e Lu´ıs Figueiredo, Functionalization of porous carbons for catalytic applications, J. Mater. Chem. A, 2013, 1, 9351–9364.
45. Hsisheng Teng, Ying-Tsung Tu, Yu-Chung Lai, Chi-Cheng Lin; Reduction of NO with NH_3 over carbon catalysts: The effects of treating carbon with H_2SO_4 and HNO_3, Carbon 2001, 39, 575–582.
46. J. L. Figueiredo, M. F. R. Pereira, M. M. A. Freitas and J. J. M. Orfao, Modification of the surface chemistry of activated carbons, Carbon, 1999, 37, 1379–1389.